

Review

Polymer/montmorillonite nanocomposites with improved thermal properties Part II. Thermal stability of montmorillonite nanocomposites based on different polymeric matrixes

A. Leszczyńska^a, J. Njuguna^b, K. Pielichowski^{a,*}, J.R. Banerjee^c

^a Department of Chemistry and Technology of Polymers, Cracow University of Technology, ul. Warszawska 24, 31-155 Kraków, Poland

^b School of Industrial and Manufacturing Science, Cranfield University, Cranfield, Bedfordshire MK43 0AL, UK

^c School of Engineering and Mathematical Sciences, City University, Northampton Square, London EC1V 0HB, UK

Received 8 December 2005; received in revised form 8 November 2006; accepted 8 November 2006

Available online 15 November 2006

Abstract

In previous part of this work factors influencing the thermal stability of polymer nanocomposite materials were indicated, such as chemical constitution of organic modifier, filler content, nanocomposites' structure and the processing-dependent degree of homogenization of nanofiller, were presented. In this part the basic changes in thermal behaviour of different polymeric matrixes (e.g. polyolefins, polyamides, poly(vinyl chloride) and styrene-containing polymers) upon addition of montmorillonite have been described. Brief description of the kinetics of the decomposition process in inert and oxidative environment, as well as analysis of volatile and condensed products of degradation, have also been presented.

© 2006 Elsevier B.V. All rights reserved.

Keywords: Polymer nanocomposites; Montmorillonite; Thermal stability; Degradation

Contents

1. Introduction	2
2. Polyolefins	2
3. Polyamides (PA)	8
4. Styrene-containing (co)polymers	10
5. Poly(methyl methacrylate) (PMMA)	15
6. Poly(vinyl chloride) (PVC)	16
7. Polyesters	17
8. Polyimide (PI)	18
9. Epoxy resins	18
10. Polyurethanes (PU)	19
11. Ethylene–propylene–diene terpolymer (EPDM)	19
12. Poly(vinyl alcohol) (PVA)	19
13. Polylactide (PLA)	20
14. Summary	20
References	20

DOI of original article: [10.1016/j.tca.2006.11.002](https://doi.org/10.1016/j.tca.2006.11.002).

* Corresponding author. Tel.: +48 12 6282727; fax: +48 12 6282038.

E-mail address: kpielich@usk.pk.edu.pl (K. Pielichowski).

1. Introduction

Polymer/clay nanocomposites preparation involves high temperatures irrespective of the fabrication route and also most polymeric materials require prolonged service in air at high temperatures. If the processing temperature is higher than the thermal stability of the organic component used for montmorillonite (MMT) modification, decomposition will take place, leading to variations in organically modified MMT (OMMT) structure as the material degrades. Thus, determination of the onset temperature of degradation, resultant products of degradation and the stability of the polymer in the presence of layered silicates as well as understanding the relationship between the molecular structure and the thermal stability (decomposition temperature, rate, and the degradation products) of the organic modifier in the galleries of layered silicate is critical [1,2].

It has been reported that some nanocomposites combining MMT and polymer matrix exhibited improved thermal stability [3,4], such as poly(methyl methacrylate) (PMMA) [5], poly(dimethylsiloxane) (PDMS) [3], polyamide (PA) [6,7] and polypropylene (PP) systems [8]. In a previous paper [9], it was noted that the introduction of layered silicates into polymer matrix may enhance its thermal stability. However, thermal behaviour of polymer/MMT nanocomposites is complicated and many factors contribute to increase in thermal resistance. Due to characteristic structure of layers in polymer matrix and nanoscopic dimensions of filler particles, several effects have been observed that can explain the changes in thermal properties. The level of surface activity may be directly influenced by the mechanical interfacial adhesion or thermal stability of organic compound used to modify montmorillonite. Thus, increasing the thermal stability of OMMT and resultant nanocomposites is one of the key points in the successful technical application of polymer/clay nanocomposites on the industrial scale. Based on recent research, our previous review provided a detailed examination of factors influencing thermal stability including the role of chemical constitution of organic modifier, composition and structure of nanocomposites and mechanisms of improvement of thermal stability in polymer/montmorillonite nanocomposites. The present work reviews thermal properties and degradation processes of nanocomposites based on different polymer matrixes. It discusses the basic changes in thermal behaviour of different polymeric matrixes (polyolefins, polyamides (PA), styrene-containing polymers, poly(methyl methacrylate) (PMMA), poly(vinyl chloride) (PVC), polyesters, polyimides (PI), epoxy resins, polyurethanes (PU), ethylene–propylene–diene terpolymer (EPDM), poly(vinyl alcohol) (PVA), and polylactide (PLA)) upon addition of montmorillonite with special focus on the influence of montmorillonite on kinetics of degradation process and formulation of condensed/volatile products in oxidative and pyrolytic conditions.

In this work, if not otherwise stated, terms like “clay content”, “filler content”, “silicate content”, “organobentonite content”, *etc.*, indicate the content of organomodified montmorillonite in nanocomposite.

2. Polyolefins

In our previous paper the thermal stability of polymeric nanocomposites was shown to be strongly dependent on the degree of MMT exfoliation/intercalation [9]. In fact, several factors were found to govern the thermal stability of nanocomposite materials, such as intrinsic thermal resistance of polymer matrix, nanofiller content, chemical constitution of organic modifier in bentonite and chemical character of polar compatibilizers as well as an access of oxygen to composite material during heating. When considering polyolefins for nanocomposites matrix, difficulties can be foreseen in dispersing the nanoadditives due to polyolefins' weak intermolecular attractions (van der Waals forces) between hydrocarbon chains of polyolefin and the octadecylammonium species of organobentonite. Therefore, when attempting to disperse MMT additional compatibilization is required to strengthen the interfacial interactions in hybrid material.

In this perspective, the use of polyethylene (PE) or polypropylene (PP) modified with polar copolymers as a matrix for nanocomposite or a compatibilizing agent has been proposed in many works to improve nanoadditive dispersion and achieve stabilizing effect of organoclay in polyolefin. For instance, Ding et al. [10] prepared PP nanocomposites compatibilized with PP solid-phase graft, where maleic anhydride, methyl methacrylate and butyl acrylate were used as the grafting co-monomers. The obtained PP nanocomposites exhibited improved thermal stability in a function of MMT content. At relatively low content of OMMT, the initial thermal stability increased, reaching a maximum at 4 phr of OMMT in nanocomposite, and then decreased when the OMMT content was higher than 4 phr. In another works [11,12] the temperature at the onset of the thermal decomposition of PP–clay nanocomposites was increased by nearly 130 °C, as compared with that of pure PP. Moreover, the weight loss curve of the PP nanocomposites was almost vertical which reflected a very rapid decomposition process. One of the goals of the research development was to obtain carbocation substituted clay with thermal stability higher than commercial ammonium-substituted clay exhibit [13]. From Fig. 1 one can see the enhanced thermal stability of the substituted tropylium cation clay—only 2% of the mass was lost at 400 °C.

Chiu et al. [14] investigated the thermal stability of PP nanocomposites with different organoclays and compatibilizers

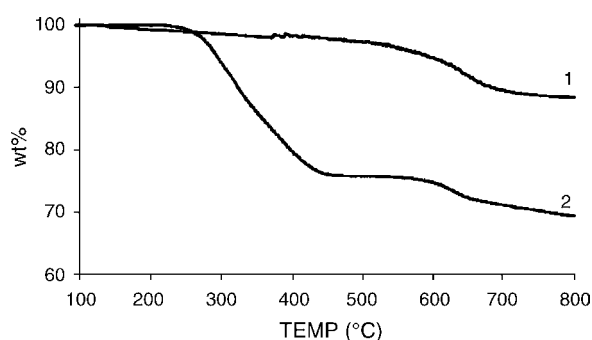
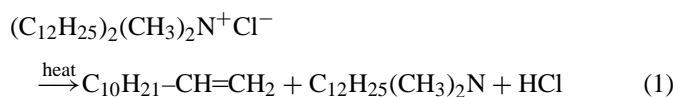
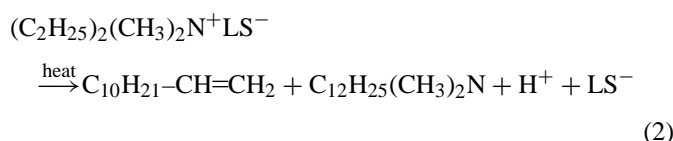


Fig. 1. TG profiles of (1) styrenetropylium clay and (2) ammonium-substituted clay [13].

(maleic anhydride grafted PP (PP-*g*-MA) or styrene-*co*-maleic anhydride oligomer (SMA)). The investigations confirmed the thermal stability enhancement of PP after adding dimethyl dihydrogenated tallow quaternary ammonium ion (DDTQA) modified clay, while for the methyl tallow bis-2-hydroxyethyl quaternary ammonium (MTHQA) containing composites thermal stability enhancement was not evident. It was pointed that the diminished thermal stability of PP was observed while MTHQA and SMA were simultaneously present in the PP matrix. On the other hand, the enhancement in thermal stability of PP/DDTQA nanocomposites became more evident as a PP-MA compatibilizer was further added with maximum enhancement occurring at 10 wt.% of compatibilizer amount. However, when protonated silicate, created as a result of decomposition of the surfactant (Eqs. (1) and (2)), interacts with co-monomers showing sensitivity to acid catalyzed degradation reactions, adverse effect is observed [15].



When quaternary cation is bonded to layered silicate (LS) surface a H^+ can be evolved:



Deacylation reaction has been postulated for reduction in initial temperature of degradation of compatibilized PP resin under non-oxidative conditions, except of ethylene-methyl acrylate-acrylic acid terpolymer modified system [16]. When octadecylammonium chloride modified clay (C18MMT) was further modified with MA in presence of diphenylamine-2-carboxylic acid as an initiator and then melt-blended with PP to obtain grafted-intercalated composites (GIC), the temperature at the onset of thermal decomposition was lower than that of polypropylene-C18MMT nanocomposites since GIC contained a large amount of clay and low-molecular-weight PP-*g*-MA, but the final decomposition temperature was higher than that of polypropylene-C18MMT nanocomposite [11].

In Qin's et al. work the kinetic analysis of degradation process of PP upon addition of MMT revealed some changes of kinetic parameters, such as reaction order and activation energy [17]. The value of reaction order n of PP nanocomposites with organomodified MMT both upon addition of compatibilizer (PP-*g*-MA) and without it was altered from 1 for pure PP to 0. The similar change of reaction order was observed for composites with protonic clay (clay intercalated at acidic sites (H^+) and denoted as H-MMT) while for Na-MMT composites n took intermediate values. The alteration of the reaction order, from first-order to zero-order, was associated with the acidic sites inherently present in H-MMT and created on heating on organically modified clay layers. The enhanced thermal stability of PP/MMT nanocomposites was connected with increased activation energy. E increased as the clay particles in the PP

matrix became smaller and more homogeneous—the highest thermal stability had the PP/PP-*g*-MA/OMMT nanocomposite. This suggested that the shielding effect of the clay layers could increase the activation energy of the thermal degradation of the polymer matrix.

Lomakin et al. studied the thermo-oxidative degradation of PP nanocomposites and, according to the kinetic analysis, PP nanocomposites had superior thermal and fireproof behaviour compared with neat PP [18]. The thermal stabilization effect of nanoclay structure in a polymer matrix was arising from a one-dimensional diffusion process of catalytic-charring throughout the second step in the thermo-oxidative degradation of PP nanocomposites. This reaction type was ascribed as responsible for the overall process of carbonization.

When sufficient energy is provided for the homolytic dissociation of bonds such as C–C, C–H or C–O, the decomposition of PP-*g*-MA *via* free radical chain reactions occurs, which may generate several products in the gas phase (e.g. acetic acid, formic acid, acetone, acetaldehyde and carbon mono- and dioxide) [19,20]. These products, due to their low molecular weights, can migrate out of the solid polymer. By using the combined TG/FTIR technique, qualitative and quantitative data concerning degradation of PP-*g*-MA with methyl tallow dihydroxyethyl ammonium modified MMT (PP-*g*-MA–MMT2EtOH) could be obtained giving some clues as to the chemistry of the reactions [21]. A detailed examination of the infrared spectra evolution of PP-*g*-MA revealed that beginning of the weight loss is caused by the evolution of hydrocarbons and carbon dioxide/monoxide. In nanocomposites, the loss of these volatile products began at different temperatures depending on the composition and continued until the weight loss was completed. The spectra of gases evolved during degradation from nanocomposites displayed the same bands as the spectrum of pure polymer, however, the intensity of absorbance for the hydrocarbons (2963 cm^{-1}) band was lower. Furthermore, a disappearance of the CO_2 bands and the bands in carbonyl region (around 1726 cm^{-1}) displaying an acid evolution was noticed on the FTIR spectrum of the corresponding PP-*g*-MA nanocomposite with *N,N,N*-trimethyloctadecylammonium (PP-*g*-MA–OD3MA) heated under N_2 (in anaerobic conditions). In this case, absorbance of the 2963 cm^{-1} band and its shoulders increased slightly. Also, for the nanocomposites blended in air and heated in a flow of air the evolved gas profile calculated *via* the Gram–Schmidt algorithm indicated a delay in the release of volatile products over the decomposition of PP-*g*-MA nanocomposites with OD3MA modified clay. These data indicated some changes in the amounts and sequences of evolution of volatile products caused by the presence of MMT, however, further investigation is needed to propose a possible mechanistic model of degradation reaction of PP-*g*-MA in a presence of OMMT.

The evolved products of polyethylene (PE) and PE/clay nanocomposite during thermal degradation consisted of hydrocarbons up to C_{31} (m/z 436) [22]. At each carbon number three components were detected by GC/MS method: α,ω -diene, 1-ene and alkane. Basically, these compounds are produced through random scission followed by disproportionation reac-

tion. Assuming that disproportionation is the only process for the termination of the degradation reaction, the ratio of (α,ω -diene):(1-alkene):(alkane) should be 1:2:1. Referring to the GC trace of virgin polyethylene, the intensity of α,ω -diene is small compared to alkane, which implies that, when polyethylene undergoes thermal degradation, some hydrogen abstraction reactions must occur in the condensed phase. In the presence of clay, some changes were observed [23]. The peaks due to the α,ω -diene structures decreased, those of alkane structures increased and other noise-like peaks corresponding to other unsaturated structures were qualitatively increased. It was proposed that the extent of the hydrogen abstraction reaction is increased qualitatively, producing more intense alkane peaks, and, more random scission occurs, which produces various unsaturated aliphatic structures having different positions for the double bond in the chain. Since the clay layers act as a barrier, the degrading molecules are confined, which leads to more extensive random scission and hydrogen abstraction.

It is acknowledgeable that different thermal behaviour of polyolefin nanocomposites was observed in inert and oxidative conditions. As a subject of the matter, studies by Adams [24] has shown that oxidation reactions create thermally weak bonds, i.e. hydroperoxides and peroxides, that can initiate the thermal degradation. Indeed, the produced hydroperoxides can decompose to propagate the oxidation process, leading to end products according to well-known oxidation mechanism. In polyethylene (PE) nanocomposites the TG data analysis revealed the delay of catastrophic weight loss under air and little stabilizing effect observed during non-oxidative degradation. The postulated effect of protective role that generated silica-rich char took part in reducing the rate of oxidative degradation in the composite materials and appeared most strikingly in the low density PE (LDPE) and poly(ethylene-*co*-methyl acrylate) (PEMA) polymer systems, due to their low inherent resistance to ambient oxygen [15]. Oxidation reactions could contribute to reduction of the thermal stability for maleic anhydride grafted PP nanocomposites (PP-*g*-MAH-MT2EtOH) produced in air as seen by the decrease of temperature at 50% mass loss ($T_{50\%}$) relative to the ones of PP-*g*-MA. On the other hand, in the case of PP-*g*-MA-OD3MA blends, oxygen did not seem to play a determinant role. This was related to the absence of a reactive group in trimethyl octadecyl ammonium (OD3MA) modified clay that could have initiated the oxidation process—a hypothesis that was confirmed by using several organically modified MMTs for systematic experiments. The first observation was that during the thermal oxidation, decomposition was enhanced by the presence of oxygen comparatively to the ones obtained over the pyrolysis. Contrary to previous development, investigations conducted by Zhang and Wilkie [25] noted little effect of the clay on the onset of non-oxidative thermal degradation in PE nanocomposites, both with and without the incorporation of maleic anhydride—Table 1.

In another interesting development, poly(ϵ -caprolactone) (PCL) and PS modified clay were used as filler for polyolefins [26]. The enhancements in the onset temperature were larger for PCL-modified clay than for the PS-modified clay. The TG curves for both PP and PE nanocomposites showed two steps

in the degradation, while the virgin polymers showed only a single step. The onset temperature was greatly enhanced for these systems and appeared that the PCL present in the clay underwent the initial degradation and this stabilized the PP and PE such that they degraded at higher temperature. Regrettably, the work failed to give any explanation for these observations. Further, Zhao et al. have investigated silane modification of MMT [27,28]. Elsewhere, a recent work have revealed improved thermal stability of melt-processed nanocomposites of PE and MMT modified with (*N*- γ -trimethoxysilane-propyl)octadecyldimethylammonium chloride (abbreviated as JSAc) [29]. It was confirmed that reactive methoxysilane groups from JSAc could react with hydroxyl groups at the edges of clay layers. The main advantage of this method in comparison to previous developments aiming at chlorosilane modification of montmorillonite was that the chemical reaction with hydroxyl groups at the edge of clay layers and the interlayer ion-exchange were carried out in one step therefore eliminating troublesome solvent disposal. For the nanocomposites of PE and MMT modified with JSAc the highest thermal stability was obtained when the content of modified filler was about 2 wt.%; for higher MMT content the T_{\max} was lower than that of pure PE.

For ethylene-vinyl acetate copolymer, EVA, the thermal decomposition starts with the elimination of acetic acid (chain stripping) in the temperature region of 300–350 °C, leaving a double bond in the chain backbone, hence EVA is converted into poly(ethylene-*co*-acetylene), which undergoes further degradation to smaller molecules at higher temperature [30]. The GC traces of virgin EVA are the same in terms of the major components and relative intensities with that of PE. There is some common degradation pathway occurring if an allylic radical is formed by random scission and, after this radical either disproportionates or abstracts hydrogen, random scission occurs at the other allylic position.

In the presence of clay, some definite differences were observed for EVA compared to those in the PE/clay system: the saturated alkane peaks (m/z 240, 254, 268 and 282) increase, while the α,ω -diene peaks (m/z 236, 250, 264 and 278) decrease or disappear, and noise-like peaks, assigned to other unsaturated structures, increase [23]. The increased production of the saturated compounds and the decreased evolution of α,ω -diene indicate that hydrogen abstraction becomes more important. The greater number of the other unsaturated structure implies that extensive random scission also is more extensive due to the presence of MMT.

Costache et al. proposed that the differences in the degradation of the nanocomposites and virgin EVA may arise from secondary reactions which the secondary allylic radicals can undergo [31]. In the case of EVA nanocomposites, the clay platelets can confine these radicals, so that recombination reactions become much more probable than in the case of virgin copolymer. For EVA, the most probable reactions are radical transfer reactions with the original polymer, from which the newly formed radicals can return to the degradation cycle, undergoing additional scissions, *etc.* Also other reactions that might take place in the case of the nanocomposite were pointed by authors as shown in Fig. 2. Cross-linked structures can

Table 1
The results of thermogravimetric analysis of selected polymeric nanocomposites

Polymer matrix	Sample code	OMMT content (%)	Type of organic modifier and compatibilizer	Atmosphere	T_{onset} (°C)	Change of T_{onset}^* (°C)	T_d (°C)	Change of T_d^* (°C)	Char of nano-composite (%)	Char of pure polymer (%)	Reference
High density polyethylene (HDPE)	PE1	1	Octadecyltrimethylammonium chloride	N ₂	468 ^{0.2}	42	480 ^{0.5}	20	–	–	[124]
Low density polyethylene (LDPE)	PE/20A	3	Cloisite 20A	N ₂	438 ^{0.1}	13	478 ^{0.5}	7	4	1	[25]
	PE/MA/30B	3	Maleic anhydride + Cloisite 30B	N ₂	432 ^{0.1}	7	478 ^{0.5}	7	4	1	[25]
	PE/Triclay II	3	Ammonium salt of the terpolymer from vinylbenzyl chloride, styrene and lauryl acrylate	N ₂	463 ^{0.1}	27	488 ^{0.5}	13	2	0	[125]
Linear low density polyethylene (LLDPE)	MMT NC2.5	2.5	Hexadecyltrimethylammonium bromide	Air	427 ^{0.2}	48	–	–	–	–	[126]
Polypropylene (PP)	2.5% MAPS/PP	2.5	Ammonium salt of oligomeric copolymer of methyl methacrylate and vinylbenzyl chloride	N ₂	333 ^{0.1}	14	424 ^{0.5}	18	2	0	[127]
	PP4	3	Octadecylammonium and 21% of maleated PP	N ₂	406 ^{0.05}	–8	457 ^{max}	17	3.7 ^a	0.8	[128]
	PP6	3	Hexadecylammonium and 21% of maleated PP	N ₂	416 ^{0.05}	2	445 ^{max}	5	1.3 ^a	0.8	[128]
	PP4	4	Hexadecyltrimethylammonium bromide	N ₂	391 ^{0.05}	55	459 ^{max}	18	4.9 ^a	2.4	[129]
Isotactic polypropylene (iPP)	PP/Triclay	8	Ammonium salt of the terpolymer from vinylbenzyl chloride, styrene and lauryl acrylate	N ₂	441 ^{0.1}	41	472 ^{0.5}	23	3	0	[125]
	QN	2.5	Nanofil 848	N ₂	424 ^{0.1}	–15	450 ^{max}	–25	1.6	0	[130]
	QN	2.5	Nanofil 848	Air	315 ^{0.1}	0	402 ^{max}	24	1.8	0	[130]
Polyamide 6 (PA 6)	PA/clay	2.5	Nanomer I.30TC	N ₂	412 ^{0.05}	10	476 ^{max}	6	1.9	0	[32]
	PA/clay	5	Nanomer I.30TC	Air	425 ^{0.05}	25	485 ^b , 625 ^c	21 8	3.9	0	[32]
Polyamide 11 (PA 11)	PA 11/clay (98/2)	2	Nanomer I.34TCN	N ₂	–	–	414 ^{max}	17	–	–	[42]
	PA 11/clay (98/2)	2	Nanomer I.34TCN	Air	–	–	413 ^{max}	20	–	–	[42]
Polystyrene (PS)	PSMMT05	5	Sodium MMT (<i>sonification</i>)	N ₂	416 ^{0.1}	53	440 ^{0.5}	31	–	–	[131]
	15%COPS/PS	15	Ammonium salt of oligomeric copolymer of styrene and vinylbenzyl chloride	N ₂	395 ^{0.1}	25	438 ^{0.5}	23	6	2	[132]
	PS+5%5AC.	5	Carbazole-based salt (<i>melt blending</i>)	N ₂	395 ^{0.1}	–14	433 ^{0.5}	–9	5	0	[133]

Table 1 (Continued)

Polymer matrix	Sample code	OMMT content (%)	Type of organic modifier and compatibilizer	Atmosphere	T_{onset} (°C)	Change of (°C)	T_d (°C)	Change of (°C)	Char of nano-composite (%)	Char of pure polymer (%)	Reference
	PS+5%5AC	5	Carbazole-based salt (<i>bulk polymerization</i>)	N ₂	416 ^{0.1}	7	462 ^{0.5}	20	6	0	[133]
	PS/Triclay	12	Ammonium salt of the terpolymer from vinylbenzyl chloride, styrene and lauryl acrylate	N ₂	420 ^{0.1}	3	470 ^{0.5}	23	5	0	[134]
	PS+10A-clay+MA	~3	Cloisite 10A + maleic anhydride	N ₂	360 ^{0.1}	31	404 ^{0.5}	29	6	2	[135]
	PS+10A salt+Na-clay+MA	~3	10A salt + sodium MMT + maleic anhydride (<i>reactive melt blending</i>)	N ₂	339 ^{0.1}	10	384 ^{0.5}	9	5	2	[135]
	PS+3% BPNC16	3	Phenylacetophenone dimethylhexadecyl ammonium salt (<i>bulk polymerization</i>)	N ₂	425 ^{0.1}	25	456 ^{0.5}	20	5	0	[136]
	PS+5% BPNC16	3	Phenylacetophenone dimethylhexadecyl ammonium salt (<i>melt blending</i>)	N ₂	414 ^{0.1}	14	452 ^{0.5}	16	2	0	[136]
High impact polystyrene (HIPS)	5%COPS/HIPS	5	Ammonium salt of oligomeric copolymer of styrene and vinylbenzyl chloride	N ₂	416 ^{0.1}	2	448 ^{0.5}	8	6	1	[132]
	HIPS/Triclay	20	Ammonium salt of the terpolymer from vinylbenzyl chloride, styrene and lauryl acrylate	N ₂	425 ^{0.1}	−15	476 ^{0.5}	12	6	0	[134]
	1% MMT+HIPS	1	Salt of methyl methacrylate oligomer (PMMA12 clay)	N ₂	402 ^{0.1}	−23	450 ^{0.5}	0	1	0	[137]
Acrylonitrile-butadiene-styrene terpolymer (ABS)	5%COPS/ABS	5	Ammonium salt of oligomeric copolymer of styrene and vinylbenzyl chloride	N ₂	400 ^{0.1}	1	435 ^{0.5}	9	7	6	[132]
	ABS/Triclay	12	Ammonium salt of the terpolymer from vinylbenzyl chloride, styrene and lauryl acrylate	N ₂	425 ^{0.1}	−5	465 ^{0.5}	10	6	1	[134]
	1% MMT+ABS	1	Salt of methyl methacrylate oligomer (PMMA12 clay)	N ₂	438 ^{0.1}	35	401 ^{0.5}	−30	2	0	[137]
Styrene-acrylonitrile copolymer (SAN)	SAN/Triclay	4	Ammonium salt of the terpolymer from vinylbenzyl chloride, styrene and lauryl acrylate	N ₂	424 ^{0.1}	0	443 ^{0.5}	−9	3	1	[134]
Poly(methyl methacrylate) (PMMA)	PMMA-33-05	15	Salt of methyl methacrylate oligomer	N ₂	351 ^{0.1}	80	397 ^{0.5}	58	8	0	[138]
	5% MAPS/PMMA	5	Ammonium salt of oligomeric copolymer of methyl methacrylate and vinylbenzyl chloride	N ₂	303 ^{0.1}	28	359 ^{0.5}	19	4	2	[127]
	PMMA/4%93A	4	Cloisite 93A	N ₂	295 ^{0.1}	24	367 ^{0.5}	58	4	0	[139]

	PMMA/4% 93A	4	Cloisite 93A	Air	297 ^{0.1}	–	368 ^{0.5}	–	5	–	[139]
	PMMA/4% phos1	4	Tributylhexadecylphosphonium	N ₂	293 ^{0.1}	22	376 ^{0.5}	67	4	0	[139]
	PMMA/4% phos2	4	Tetraphenylphosphonium	N ₂	285 ^{0.1}	14	368 ^{0.5}	59	5	0	[139]
	PMMA/MMT	0.8	Sodium MMT after purification and sonification	N ₂	355 ^{0.1}	106	–	–	–	–	[78]
Poly(vinyl chloride) (PVC)	PVC/MMT-1	1	<i>N</i> -[4-(4'-Aminophenyl)]phenyl phthalimide	N ₂	293	5	–	–	–	–	[81]
	PVC/MMT-16C	1	1-Hexadecylamine	N ₂	290	2	–	–	–	–	[81]
Poly(ethyl terephthalate) (PET)	C ₁₂ PPh-MMT/PET	3	Dodecyltriphenylphosphonium chloride	N ₂	386 ^{0.02}	16	–	–	21	1	[140]
Sulfonated poly(ethyl terephthalate) (SPET)	SPET6M5	5	Hexadecyltrimethylammonium chloride	N ₂	357 ^{0.1}	69	–	–	11.8	1.4	[141]
Poly(butyl terephthalate) (PBT)	PBT2	3	Hexadecyltrimethylammonium chloride	N ₂	366 ^{0.03}	–5	404 ^{max}	–3	2.03 ^a	5.27	[89]
	PBT3	3	Cetylpyridinium chloride	N ₂	370 ^{0.03}	–1	407 ^{max}	0	7.05 ^a	5.27	[89]
Poly(trimethylene terephthalate) (PTT)	PTT/11K-P	5	Cetyltrimethylammonium chloride	N ₂	–	–	401	2	8.1	0.3	[142]
Poly(ethylene terephthalate- <i>co</i> -ethylene naphthalate) (PETN)	PETN/4% clay	4	Hexadecyl amine	N ₂	418 ^{0.02}	14	454 ^{max}	1	17	12	[91]
Poly(etherimide) (PEI)	PEI/MMT	5	<i>N</i> -[4-(4'-Aminophenyl)]phenyl phthalimide	N ₂	526 ^{0.05}	6	–	–	–	–	[143]
Polyimide (PI)	PI/C12-MMT	6	Dodecylamine	N ₂	604	15	665 ^{max}	32	65	64	[147]
Epoxy resin	TGDDM 5% OLS	5	Nanomer® I.30E	N ₂	349 ^d	4	377.6 ^d	2.7	19.9	15.7	[100]
Polyurethane (PU)	PU/clay 5 wt.%	5	Cloisite 30B (<i>PU polyether based</i>)	–	289 ^{0.05}	10	382 ^{max}	23	3.47	0.19	[144]
	PU/DTA-MMT	4	Dodecyltrimethylammonium chloride	–	322	18	433	8	8	5	[145]
	3OH-Mont/PU39	1	Trishydroxymethyl aminomethane	N ₂	348 ^{0.05}	40	384.1 ^b , 460.7 ^c	–37.2, 116.0	–	–	[146]
Poly(vinyl alcohol) (PVA)	CLVA5	5	Diallylammonium chloride	N ₂	–	–	270 ^{max}	40	15.0	5.4	[116]

Superscript max: temperature at maximum rate of mass loss; superscripts 0.02, 0.03, 0.05, 0.1, 0.5: the temperature at which 2, 3, 5, 10 and 50% mass loss occurred, respectively; *: in comparison with pure polymer.

^a The char for organic modified MMT at 600 °C has already been subtracted.

^b Temperature at maximum rate of mass loss during the first stage of degradation.

^c Temperature at maximum rate of mass loss during the second stage of degradation.

^d Onset temperature of degradation.

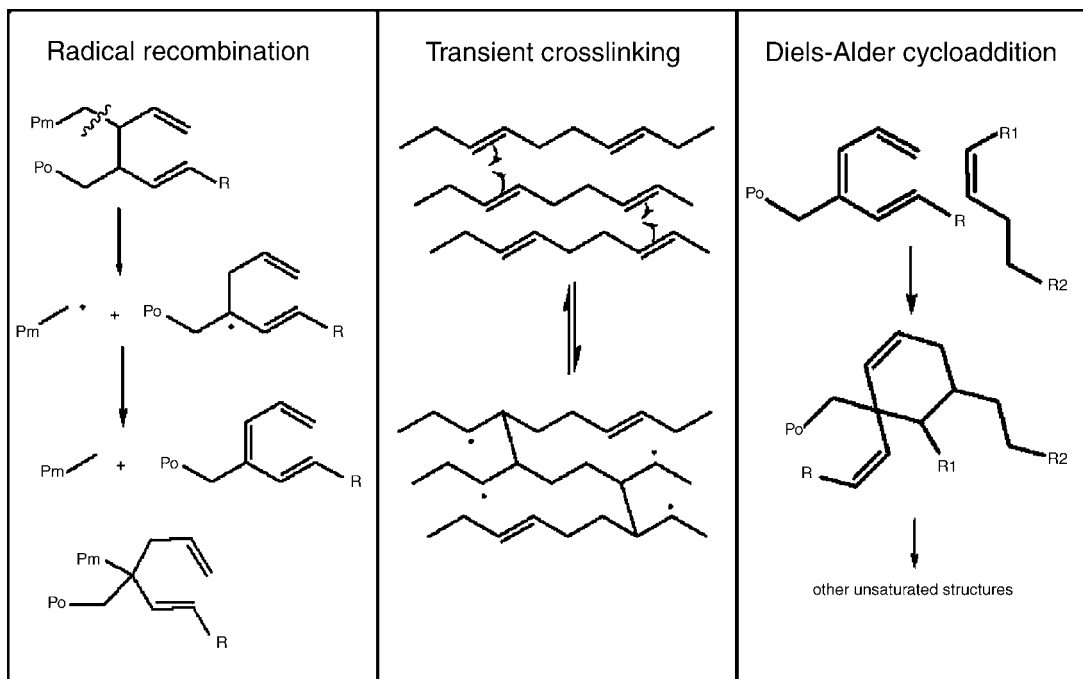


Fig. 2. Reactions favoured in the presence of clay during thermal degradation of EVA [31].

undergo further scissions, leading to the formation of radical species which can either disproportionate, producing various branched trienes, or recombine, forming other cross-linked structures and/or internal olefins. Linear polymer chains which have a favourable orientation promoted by clay confinement can undergo transient cross-linking. In addition, the trienes formed can undergo Diels–Alder cycloaddition reactions leading to cyclic structures and possibly, upon hydrogen abstraction, to other unsaturated structures. All these cross-linked, branched or multiple double bonds containing structures can explain the increased thermal stability of the nanocomposite observed by TGA, since more energy is required to break the additional bonds formed.

3. Polyamides (PA)

Pramoda et al. [32] investigated the volatile products from PA 6 nanocomposites degradation. The FTIR spectrum of the evolved gases from PA 6 nanocomposites in N_2 atmosphere showed the production of water, CO_2 and an olefinic compound. Absorption bands were also observed at 1653 , 1772 , 3331 cm^{-1} and assigned to amide, carboxylic acid, and hydroxyl functional groups, respectively. However, the absorption at 1653 cm^{-1} did not correspond to the amide functional group of poly(ϵ -caprolactam) oligomers but rather to ϵ -caprolactam monomer in agreement with the published data [33,34]. The IR spectra showed the evolution of NH_3 (970 cm^{-1}) at the same temperature range as that of the organic fragments released, indicating the presence of the decomposition reactions in the organically modified layered silicate systems during heating. The evolution of gas products from PA 6 nanocomposites in air started at around 340°C and increased gradually to a maximum at 485°C , before decreasing. The majority of the gas evolution ended at

520°C and thereafter only CO_2 appeared along with the traces of other gas products. However, the major degradation product was CO_2 in all cases. The CO_2 evolution was related to the cleavage of C–N amide bond and the alkyl chain oxidation. Apart from CO_2 other peaks suggested the presence of NH, OH and the cleavage of alkyl chain and existence of CH_3 , CH_2 and NH_3 fragments. The presence of CO was indicated at 2280 cm^{-1} by its characteristic double bands. These peaks appeared almost simultaneously together with CO_2 indicating the cleavage and oxidation of alkyl chains. However, for the PA 6 with 2.5 wt.% clay there was another maximum of CO_2 volume at 625°C , implying the intense oxidation of organic products in air. Further, TG curve indicated that a weak but clear second decomposition peak was present under air.

TG investigations on the thermal degradation of PA 6/clay showed that while single stage decomposition was found in the N_2 atmosphere, double-stage decomposition (as evidenced by a shoulder/peak at 630°C) was found in the air atmosphere for nanocomposites containing 2.5 wt.% of organomodified MMT [32]. The degradation trends in N_2 environment for both PA 6 and PA 6/clay (2.5 wt.%) nanocomposites were similar but the residues left behind after decomposition were different. While there was practically no residue left for PA 6, in the case of PA 6/clay (2.5 wt.%) nanocomposites it was found to be 1.9% under nitrogen. The onset temperature of degradation was about 10°C higher for nanocomposite with 2.5 wt.% clay additions than that for neat PA 6. This indicated that PA 6/clay (2.5 wt.%) nanocomposites had greater thermal stability than the pure PA 6, which was contrary to previous results obtained by Gilman et al. [35]. These findings were related to morphological observations that showed exfoliated structure only for 2.5 wt.% clay, and distinct clay agglomerations in nanocomposites with higher clay loadings [36]. Most importantly, the study suggested that

only exfoliated polymer nanocomposites exhibited improved thermal stability and that agglomerated clay particles did not significantly affect the thermal stability of the polymer matrix.

Vapour phase FTIR data can be supported by GC analysis, as it was done in recent work of Jang and co-workers on polyamide-based nanomaterials. The main degradation product of PA 6 detected by GC/MS method was ϵ -caprolactam (m/z 113) [37,38]. Monomer is produced mainly through end-chain acidolysis and aminolysis. The other evolved products correspond to linear structures, which are produced by chain scission and hydrolysis of amide linkage. In the presence of clay there were no significant differences found in the evolved products by FTIR method in terms of the peak positions [39]. However, the GC traces of the evolved products during thermal degradation of PA 6 nanocomposites showed more intense peaks for the linear compounds with less intense evolution of ϵ -caprolactam—Fig. 3. Furthermore, the viscosity of residual condensed phase dissolved in formic acid increased with an increasing clay content which indicates that more extensive random scission and inter-chain aminolysis or acidolysis have occurred. It was argued that inter-chain reactions become significant in the presence of clay

because the degrading polymer chains are trapped in the gallery space of the clay during thermal degradation (Fig. 4).

Generally, the thermal stability of PA 6/MMT nanocomposites in terms of initial temperature of decomposition (T_{id}) was slightly increased [32] or remained the same [40,41].

Thermal degradation studies on PA 11/organoclay nanocomposites clearly showed that the onset of decomposition temperature (at sample mass loss of 5 wt.%) was significantly improved by about 20 °C at low nanofiller concentrations (<4 wt.%) and quickly levelled off, especially in air flow [42]. In contrast, at high clay content (8 wt.%), the (intercalated) nanocomposite degraded at temperature 5–10 °C inferior to the degradation of the pure unfilled PA 11 matrix.

Qin et al. [6] presented on thermal stability and flammability of PA 66/MMT nanocomposites. The TG profiles of pure PA 66, OMMT nanocomposite and MMT microcomposite in nitrogen and air environments showed that the nanocomposite had a higher decomposition temperature (435 °C in nitrogen and 450 °C in air) than the microcomposite (425 °C in nitrogen and 440 °C in air). Interestingly, when compared to the pristine polymer, the decomposition temperature of the nanocomposite was

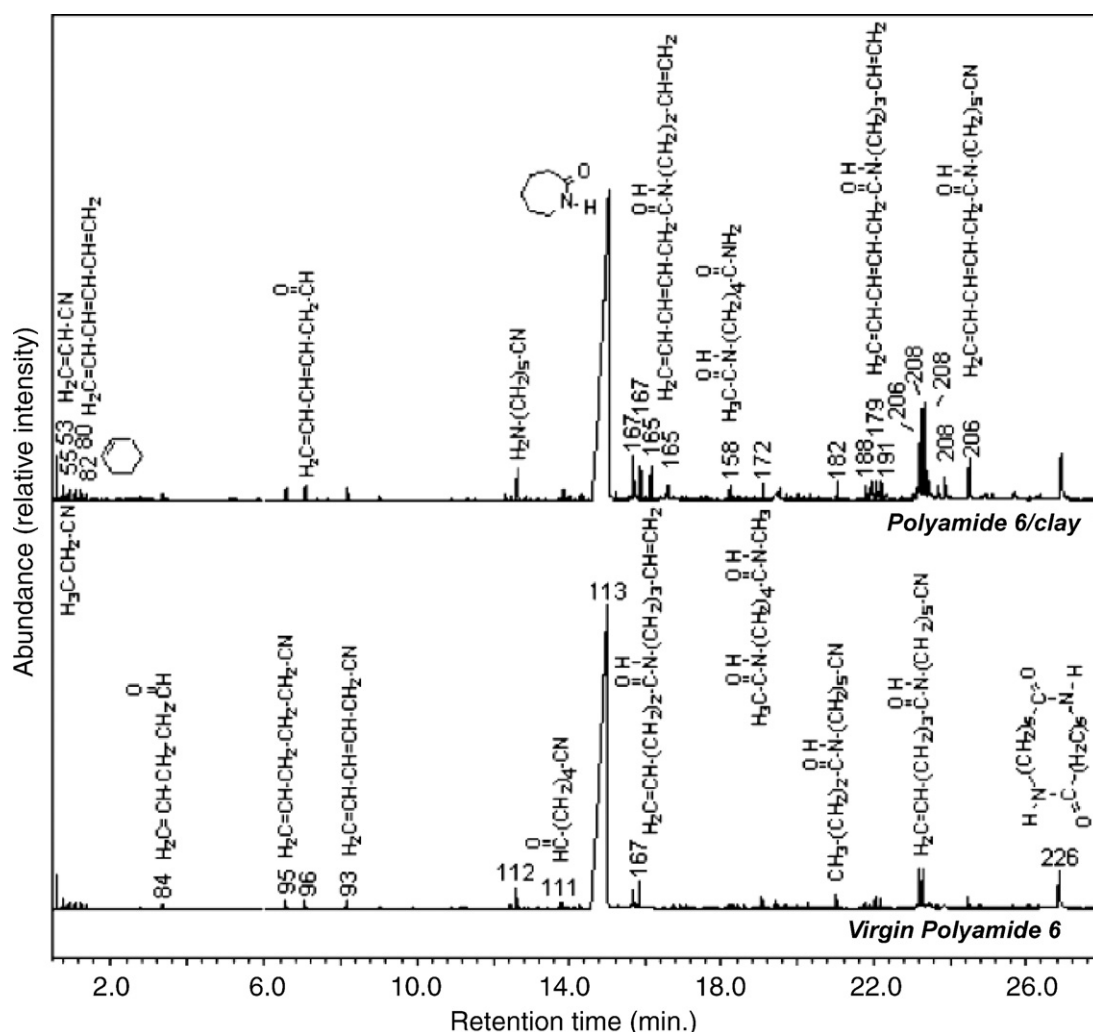


Fig. 3. GC traces of virgin polyamide 6 and its clay nanocomposite. Inset number denotes m/z in mass spectrum of each peak. The inset structures correspond to each peak of GC trace [39].

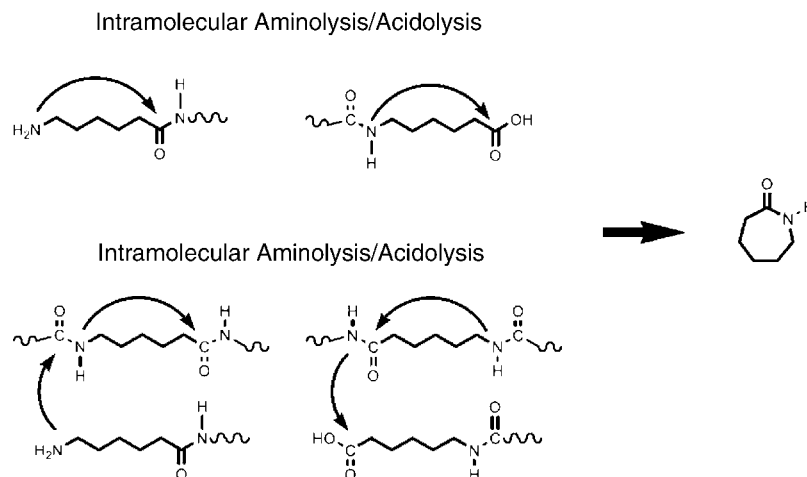


Fig. 4. Inter and intra-molecular reactions in PA 6 [39].

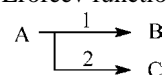
10 °C lower than the pure PA 66 in nitrogen atmosphere but more than 5 °C higher than the pure PA 66 in air atmosphere. The difference was related to the absence or presence of oxygen. The thermal behaviour of the nanocomposites in N₂ atmosphere indicated that the addition of MMT accelerated the thermal decomposition of PA 66 matrix, a fact the researchers associated to the catalysis of water evolved from MMT (adsorbed or from dehydroxylation). In oxidative atmosphere, the degradation was mainly oxygenolysis and the barrier effect of the silicate layers was dominant due to the formation of carbonaceous-silicate char on the surface of nanocomposite. Therefore, the nanocomposites had a higher thermal stability than pure PA 66 in air.

4. Styrene-containing (co)polymers

Bourbigot et al. [43] showed that the routes of thermal degradation of PS/MMT nanocomposites differ in pyrolytic and oxidative conditions. Both in inert atmosphere and in oxidative conditions at around 200 °C small weight loss was observed (for nanocomposite containing 1.5 wt.% of OMMT) that was assigned to degradation of the organomodifier of the clay. Under pyrolytic conditions the thermal stability of nanocomposites was enhanced in terms of the onset temperature of degradation, which was 50 °C higher compared to pure PS. Under thermo-oxidative conditions the degradation of pure polymer and its nanocomposite occurred at the comparable temperatures but the charring significantly increased for the PS/MMT nanocomposites—from 5 to 15% at 400 °C. At higher temperatures it underwent further degradation resulting in 2% final residue in both oxidative and pyrolytic conditions—this was assigned to the mineral content of MMT in nanocomposites (Fig. 5). It was confirmed that the degradation of polymeric materials in inert gas occurred in higher temperature ranges than the process led in air atmosphere. For virgin PS the onset temperature of the main degradation in nitrogen was 30 °C higher while for PS nanocomposites it was 100 °C higher than the temperatures of thermo-oxidative degradation. In the case of thermo-oxidative degradation the role of MMT was explained in terms of promoting the char formation.

For the thermal degradation of PS and PS/MMT nanocomposites under inert atmosphere, the shape of TG curves and their derivatives suggested a degradation in one-step reaction, but the evolution of the shape as a function of the heating rate was an indication of complex reactions. The kinetic analysis of the thermal degradation of PS and PS/MMT nanocomposites has been used to prove the complex character of that process in pyrolytic conditions. The researchers used Friedman analysis as a preliminary step of the kinetic analysis. This approach provided the plot of the activation energy versus the fractional weight loss. The kinetic analysis revealed that both for the pure PS and its nanocomposites the activation energy was not constant but grew from 80 to about 200 kJ/mol (Fig. 6) indicating that the degradation did not take place as a one-step reaction but as multi-step reactions.

The highest quality of fit for pristine PS gave two competitive reactions with Avrami–Erofeev functions:



The pyrolysis of PS produces mainly styrene monomer and some oligomers of styrene (dimer, trimer, tetramer and pentamer) [44–46]. The proposed mechanism is thermal scission of the polymer chain, which yields primary radical species.

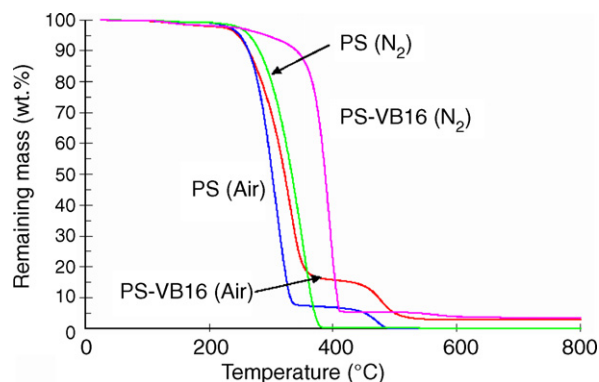


Fig. 5. TG profiles of PS and PS-VB16 in pyrolytic and thermo-oxidative conditions (heating rate 1 K/min) [43].

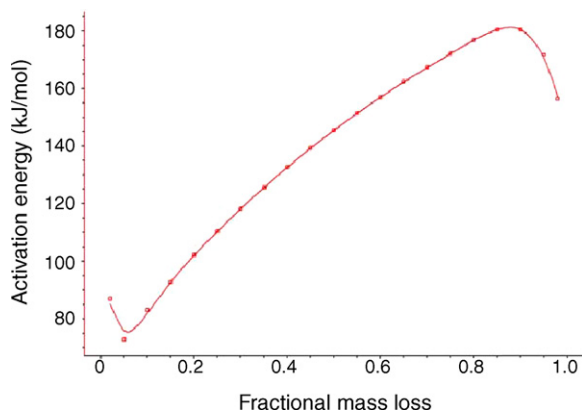
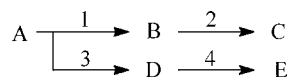


Fig. 6. Activation energy of pure PS vs. fractional mass loss determined using the Friedman analysis (nitrogen flow) [43].

Oligomers are produced *via* intramolecular radical transfer reactions. The reaction 1 in chosen model could be assigned to the random scission of the polymeric chains since the activation energy calculated by ‘model-fitting’ method using Avrami–Erofeev model were approximately equal to the expected value of activation energy of PS chain scission. The other reactions involved in the pyrolysis of PS were end-chain and mid-chain β -scission, radical recombination and hydrogen transfer. All these reactions have relatively low activation energies (between 40 and 120 kJ/mol) and were assigned to reaction 2 of the model proposed. Since the true reactions of the system are too complex to be characterized in any fundamental way, the reactions in models of thermal degradation were described as pseudo (or lumped) species which are themselves complex materials or a mixture.

As a result of Friedman analysis the researchers found activation energy of nanocomposites climbing from 80 to 200 kJ/mol and then remaining constant. The final part of the curve was chaotic; the activation energy varied from 160 to 240 kJ/mol. This indicated that the degradation of nanocomposites occurs *via* complex reactions and supports the idea of competitive reaction. In the case of pyrolytic degradation of nanocomposites the model based on two successive reactions of two competitive reactions with Avrami–Erofeev functions showed goodness of fit.



During the first degradation step, nanocomposites exhibited kinetic parameters close to those of pure PS. Nevertheless, the significant difference between the two frequency factors of reaction 3 was found, suggesting that the probability of end-chain and mid-chain β -scission, radical recombination and hydrogen transfer reactions might be decreased in nanocomposites. This phenomenon was used to explain the enhancement of the thermal stability of nanocomposites.

Second, the thermo-oxidative degradation of PS/MMT have been investigated [43]. Again, on the basis of the evolution of activation energy according to the Friedman analysis the thermo-oxidative degradation of pristine polymer and its nanocomposites was found to be a complex process with

competitive reactions involved. Furthermore, a fact that the intermediate char yield strongly depends on the heating rate was an evidence of competitive reactions. According to the conclusions of the Friedman analysis, the degradation of the PS/MMT nanocomposites in thermo-oxidative conditions was modelled using two successive/competitive reactions with n th order functions. The determined activation energies of nanocomposite were lower than those of PS, except for reaction 3. It was interpreted in terms of (i) occurrence of oxygen initiated depolymerization of PS—the presence of the clay in PS lowered the energy of this reaction (reaction 1); (ii) as a result of the MMT presence the activation energy of reaction 3 grew (a competitive reaction with reaction 1) and higher char weights were gained, suggesting that the clay plays the role of char promoter; (iii) reactions 2 and 4 corresponded to char oxidation. The activation energies of reactions 2 and 4 of nanocomposites compared to pure PS were similar suggesting the same type of reaction. The degradation of the two systems starts at the same time but the degradation rate of PS is faster than that of the nanocomposite.

Vyazovkin et al. [47–49] employed an advanced isoconversional method in order to obtain reliable kinetic information on the thermal and thermo-oxidative degradation of a PS–clay nanocomposite, prepared by intercalating a monocationic free radical initiator into the MMT clay and the subsequent solution surface-initiated polymerization (SIP), where the PS chain growth was initiated *in situ* from the clay surface. It has been found that the introduction of the clay phase into PS causes a considerable increase in the effective activation energy of degradation. This result can be explained by the barrier model, but also by a changed concentration distribution of degradation products and/or formation of some new volatile products. Such suggestion appears to correlate with the results of cone calorimetry experiments [50] which indicate that the clay-enhanced PS composites tend to burn with the release of a significantly smaller amount of total heat. This may be because the concentration distribution of the polymer degradation products for the clay-containing PS changes toward the formation of less combustible products. In a subsequent study, Py–GC–MS and TG–FTIR techniques were applied to investigate the thermal degradation mechanism of PS nanocomposite; two main differences in mass and IR spectra of PS-based nanocomposite in comparison with those of pristine PS were observed, confirming formation of significant amounts of α -methylstyrene and dimer and trimer derivatives in PS–clay system [47]. α -Methylstyrene is formed by intermolecular transfer reactions—the key step in this mechanism is hydrogen transfer from one chain to another, which yields a mid-chain radical whose scission produces an unsaturated chain end, β -scission of the latter yields an α -methylstyrene by hydrogen abstraction. Because of the large correlation distance in the regular PS melt, the probability of the aforementioned intermolecular hydrogen transfer is low and so is the yield of α -methylstyrene. Conversely, the yield is increased in the ‘brush melt’ where the correlation distance is reduced to the inter-chain distance between the aligned grafted chains. Generally, the conceptual model that links the enhancement of intermolecular interactions to the formation of brush structure allows one to combine the

mechanistic aspects of degradation with the nanoscale structure and chain mobility of grafted polymer–clay systems.

Syndiotactic PS (s-PS) has received considerable attention because it is regarded as a new low-cost engineering polymer with various desirable properties. Although the nanocomposite formation of s-PS with organoclays promises to further extend the material properties of the polymer, the fabrication of such nanocomposites by direct melt-intercalation of s-PS into commercial organically treated clays was problematic, mostly because of the thermal degradation of the available organic surfactants (typically alkyl-ammoniums and to a lesser extent phosphoniums), which decompose far below the high temperatures employed for the melt processing of s-PS. Studies by Zhu on s-PS nanocomposites where montmorillonite modified with ammonium cations was used indicated that the temperature at which 10% degradation occurs was increased by 40–50 °C, independent of the fraction of clay over the range of 0.1–5%. The value for 50% degradation was typically 20–40 °C higher and indicated some dependence on the fraction of clay with larger enhancements at higher amounts of clay [51–53]. Insufficient thermal stability of organoclays and subsequent degradation of organic cations in montmorillonite galleries during processing usually caused difficulties in filler dispersing and generated contaminations influencing the final composition properties. On the other hand, when monoalkyl- and dialkyl-imidazolium surfactants were used to prepare organically modified montmorillonites with markedly improved thermal stability in comparison with their alkyl-ammonium equivalents (the decomposition temperatures increased by *ca.* 100 °C), a formation of s-PS/imidazolium-montmorillonite nanocomposites was possible even under static melt-intercalation conditions in the absence of high shear rates or solvents [54].

In Su and Wilkie development [55] new organomodifier containing vinylbenzyl groups was obtained and applied in synthesis of polystyrene and poly(methyl methacrylate) nanocomposites. Since the surfactant used for MMT modification contained vinyl group, the chemical coupling of polymer with surfactant molecules was expected during *in situ* polymerization of monomer. As a result, the onset temperature of the degradation increased by about 50 °C for PS–clay nanocomposites and between 50 and 100 °C for PMMA–clay nanocomposites. Interesting results were obtained from the TGA performed on the insoluble material extracted from these nanocomposites. This consisted of the clay along with the polymer polymerized onto the clay. The mass fraction of material that was non-volatile at 600 °C was 32% for the nanocomposite containing 0.5 wt.% of organomodified montmorillonite, 29% for the nanocomposite containing 3 wt.% of OMMT, and 21% for the nanocomposite containing 5 wt.% of clay, while the clay itself gave an 80% residue at 600 °C. These data allowed for calculation that in the nanocomposite containing 0.5 wt.% of clay the same fraction of polymer was grafted onto clay, 3.6 wt.% of polymer was bound in the nanocomposite containing 3 wt.% of clay, and 10.4 wt.% of polymer was incorporated into the 5% nanocomposite.

Recently, Wang and Wilkie [56] have investigated triphenylhexadecylstibonium trifluoromethylsulfonate that had been prepared and ion-exchanged with Na⁺-MMT to obtain new

organically modified clay. The clay had higher thermal stability than ammonium clay—only a portion of the alkyl chain was lost during degradation and all of the antimony was retained. This clay was then used to prepare a PS nanocomposite in which the clay was found not uniformly distributed throughout the polymer. However, the thermal stability of the PS nanocomposite was enhanced in that the onset temperature of the degradation, as measured by the temperature at which 10% mass was lost, was increased by 50 °C. Also, the mid-point of the degradation was found 50 °C higher for the nanocomposite than for virgin PS. All in all, the thermal stability of the PS nanocomposite investigated was quite comparable to what was observed for ammonium clay nanocomposites.

In the case of virgin PS, the degradation pathway is chain scission followed by β -scission (depolymerization), producing styrene monomer, dimer and trimer through an intra-chain reaction [57–61]. The clay affects the degradation behaviour of polystyrene and a number of additional structures is formed [62]. The comparison of collected FTIR spectra of gases evolved during degradation of pure PS and its nanocomposites allowed to notice that some products having phenyl alkene unit have been lost, while some saturated structures appeared. For the polystyrene nanocomposites a gradual increases in the intensity of the sp^3 carbon–hydrogen stretching vibration occurred as the clay content increases, especially at 2970 cm^{-1} , which was assigned as the sp^3 β carbon–hydrogen (methyl) stretching. The carbon–carbon double bond stretching at 1630 cm^{-1} and the C–H out-of-plane deformations at 990 and 910 cm^{-1} decreased with the clay content. For the pure PS, the FTIR spectra of vapour phase recorded as a function of mass loss showed no difference in the peak positions and their relative intensities, which means that the thermally degraded products were qualitatively the same from the beginning to the end stage of polymer degradation.

More specific information about the chemical composition of the evolved products was given by GC/MS method. In the presence of clay, except the styrene monomer (m/z 104), dimer (m/z 208), and trimer (m/z 312) typically produced during PS degradation, several additional structures were identified. The additional products, e.g. some head-to-head structures, were thought to be produced *via* radical recombination reaction followed by extensive random chain scission. Fig. 7 shows a proposed pathway for the radical recombination reactions. It was thought that through random chain scission and radical transfer, four radicals, denoted as A, B, C and D, might be produced. Considering the abundance and stability of radicals, A, C and D were thought to be the most abundant radicals in the degradation of polystyrene nanocomposites. In the case of the PS nanocomposite, due to the barrier effect of the clay layers, the radicals which were produced through chain scission are trapped between the clay layers and have more opportunity to undergo radical transfer and recombination reactions. In the well dispersed nanocomposite a superheated environment was probable to occur in the interior part of the nanocomposite when surrounding temperature keeps increasing during the TG run so some radicals and recombined molecules could undergo extensive random chain scission at any methylene linkages followed by

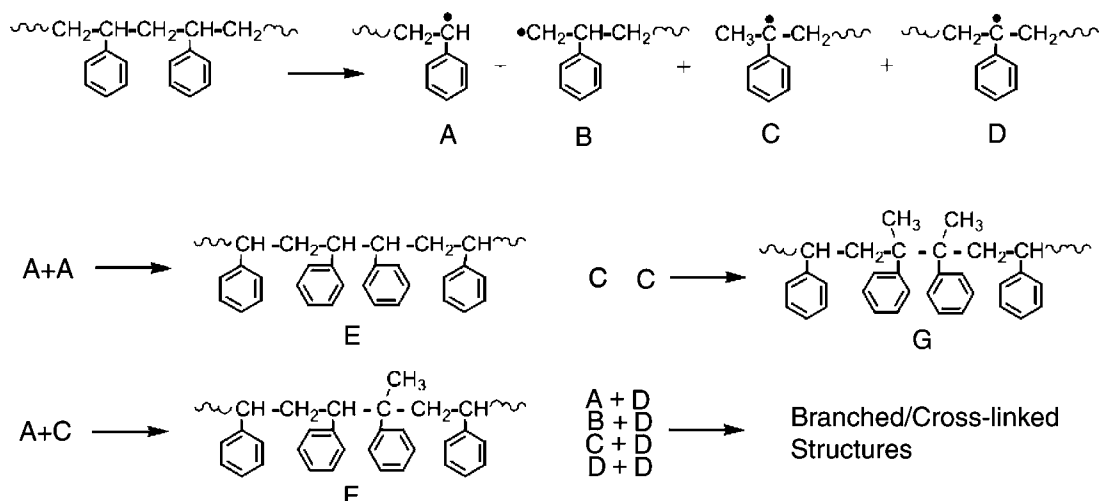


Fig. 7. Head-to-head compounds in volatile products of PS/MMT nanocomposites degradation arising from radical recombination reactions [62].

β -scission, disproportionation or hydrogen abstraction, evolving various structures—Fig. 8.

If β -scission occurs, the evolved products contain unsaturation in every molecule. Disproportionation produces molecules that exhibit both unsaturation and saturation. Hydrogen abstraction, presumably from the condensed phase, causes the production of more saturated structures. Hence, significant production of 1,3-diphenyl propane was mainly through disproportionation due to the effect of clay presence.

Additionally, the colour and viscosity changes gave some information about the chemistry of PS nanocomposite degradation. In the presence of clay, the colour of solid residues darkened as the clay content increased. Hence, cross-linking, conjugated double bond formation or carbonization, in the presence of clay could contribute to colour formation. However, the cross-linking reactions could not be an important factor since the viscosity of soluble fraction of solid residue after 40% mass loss decreased as

the clay content increased. Most probably, the conjugated double bond formation contributed to the dark colour of the residues of the PS nanocomposites and was an intermediate stage on the way to carbonization.

Wang et al. [63] have prepared acrylonitrile–butadiene–styrene terpolymer (ABS)/clay nanocomposites using a direct melt-intercalation technique. High resolution transmission electron microscopy (HTEM) results showed the ABS/clay nanocomposites to be of intercalated-delaminated structure. The nanocomposites were found to enhance the formation of char, but the onset of weight loss of ABS/clay nanocomposites occurred at a lower temperature in comparison to neat ABS. This was partly blamed on the degradation of OMMT at lower temperature than that of pure ABS (Fig. 9).

ABS/clay nanocomposites gave a larger residue from the first step of degradation—ABS has 86 wt.% mass loss, while ABS/clay nanocomposites had 9 wt.% less mass loss than

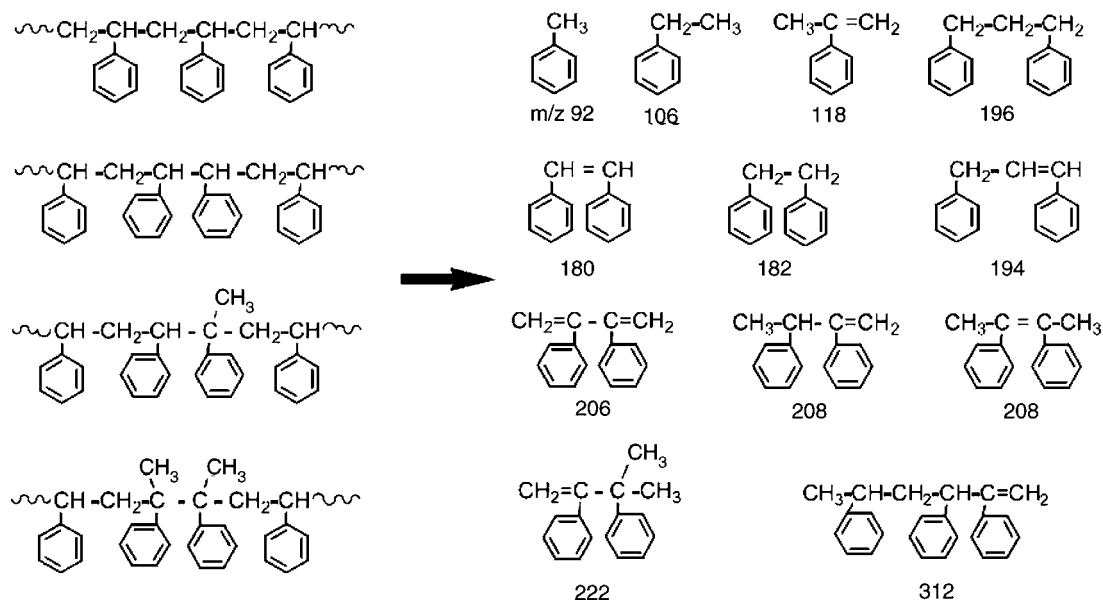


Fig. 8. Selected degradation products identified during PS/MMT nanocomposites degradation [62].

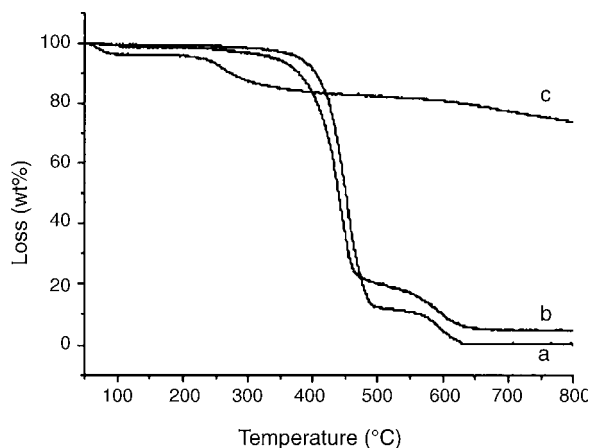


Fig. 9. TG curves: (a) ABS; (b) nanoABS; (c) OMT [63].

that of pure ABS. It was further reported that after pyrolysis the nanocomposites formed a char with a multilayered carbonaceous-silicate structure. XRD results, shown in Fig. 10, proved that the inorganic material still kept a multilayered structure at 600 °C. This high-performance carbonaceous-silicate char built up on the surface during burning—it insulated the underlying material and slowed the escape of the volatile products generated during decomposition. In the second step (500–650 °C), the relative loss of ABS/clay nanocomposite was 72%—far less than that of original ABS, 98%. Thus, it was assumed that the formation of the intercalated structure also influenced the second degradation step of ABS/clay nanocomposite in the char layer, and enhanced the stability of the ABS matrix. Elsewhere, during investigations on properties of styrene-butadiene rubber (SBR) clay nanocomposites Zhang et al. [64] observed that the thermal decomposition temperatures of nanocomposites were higher comparing to pure polymer, however this advantageous effect tend to decrease when increasing the clay content from 3 to 4 wt.%. According to authors this might be attributed to the slight phase separation with further introduction of OMMT.

In another study concerning styrene-acrylonitrile copolymer (SAN) nanocomposites researchers looked into different organic

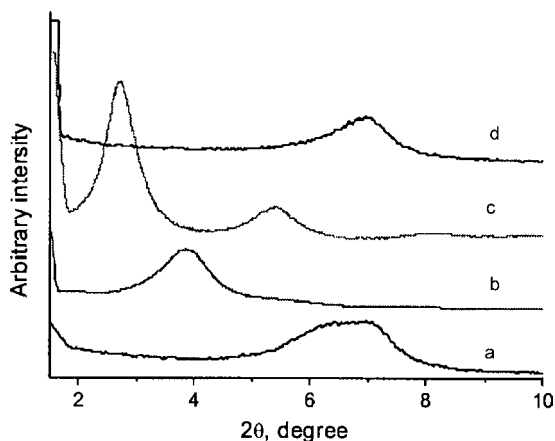


Fig. 10. XRD patterns: (a) MMT, pristine sodium montmorillonite; (b) OMT, modified clay; (c) nanoABS; (d) residue of nanoABS over 600 °C [63].

treatments differing in polarity and thermal stability. As a more thermal stable modifier for MMT than alkyl-ammonium salts (e.g. dimethyl bis(hydrogenated tallow) ammonium (DMHTA), methyl tallow bis-2-hydroxyethyl ammonium (MTBHA)), aromatic triphenyl *n*-hexadecyl phosphonium (TPHDP) and 1,2-dimethyl-3-*n*-hexadecyl imidazolium (DMHDI) were applied [65]. Most of the SAN nanocomposites exhibited better thermal stability than pristine SAN, namely; lower mass loss rate and higher decomposition peak temperature. The MMT introduction improved the thermal stability at higher temperature, however, it caused adverse effect on thermal stability at lower temperature. The TG data showed that all nanocomposites had a slightly early onset of decomposition. This was ascribed to the residual (excess) organic treatment on the clay surface. It might also be due to thermal instability of the organic treatment, as alkyl-ammonium treatments are known to undergo degradation according to Hofmann mechanism around 200 °C. Curiously enough, SAN nanocomposites made with MTBHA, DMHTA, and TPHDP treated fluorinated synthetic mica (FSM) or MMT had equivalent thermal stability. When only the clays were analysed, the alkyl-ammonium treated materials (MTBHA, DMHTA) showed the Hofmann's type of degradation behaviour at 200 °C, whereby TPHDP and DMHDI clays showed onsets of decomposition around 225 and 240 °C, respectively.

An interesting observation was made on SAN nanocomposite materials in the TG test showing whether or not the materials tested held their shape during the test and connected to the degree of nanoparticles dispersion in the SAN matrix. Materials analysed by TG had held their shape and were validated by XRD and TEM data that showed then to be well-dispersed nanocomposites. And vice versa, materials that did not hold their shape were either microcomposites, or poorly dispersed nanocomposites. To study the effect of acrylonitrile content in SAN nanocomposites, the clay dispersion and thermal stability of two additional nanocomposites based on SAN copolymers containing less acrylonitrile (AN) content (15 and 23%, respectively) were investigated. The analysis of structural features of nanocomposites, in principle, confirmed the hypothesis that while the DMHDI organic treatment preferred to interface favourably with the phenyl ring in the styrene part of the SAN backbone, it did not prefer to interface with the polar acrylonitrile part of the SAN backbone, since TPHDP–MMT dispersed poorly in these SAN resins compared with full 31% AN content SAN. Moreover, the TPHDP–MMT also showed a collapse of the organoclay interlayer distance suggesting that these materials are most likely microcomposites. To the researchers it seemed that poor dispersion of MMT in this material induced thermal degradation at temperatures lower than observed for other nanocomposites and even for pure SAN.

According to the results of *in situ* vapour phase FTIR investigation the main evolved gas products contained vinyl, nitrile, and mono substituted benzene groups, along with some aliphatic chains. The collected spectra implied that there were no differences in terms of functionality upon the formation of the nanocomposites. When studied by using the GC/MS method, the degradation behaviour of pure SAN seemed very similar to polystyrene, which is chain scission followed by β -scission [66],

producing monomers (m/z 53, 104), dimers (m/z 157, 208) and trimers (m/z 210, 261, 312). The degradation pathway of SAN in its nanocomposites with MMT exhibits more extensive random chain scission, yielding additional compounds having an odd number of carbons in the chain backbones (m/z 118, 173, 196), and radical recombination, producing head-to-head structures (m/z 236, isomers of m/z 261, etc.), but the peak intensities of the recombined products were smaller than those of polystyrene [67]. This trend may be caused by differences in the radical stability between degrading SAN and PS. The tertiary radical adjacent to benzene ring is thought to be more stable than that adjacent to nitrile group [68], hence, as soon as the latter is produced, it undergoes either radical transfer (hydrogen transfer) or β -scission, producing relatively large amounts of dimers and trimers compared to polystyrene. On the other hand, the radical adjacent to benzene ring is one of the more stable radicals, so it has more opportunity to undergo recombination reaction.

5. Poly(methyl methacrylate) (PMMA)

It is generally accepted that the decomposition of radically polymerized PMMA in nitrogen atmosphere consists of three stages: the first (100–200 °C) is ascribed to the rupture of weak head-to-head linkages in the main chain, the second (200–300 °C) is terminal vinyl group decomposition, and the third (300–400 °C) is due to the random scission of polymer main chain [69]. While decomposing in the presence of oxygen, the first peak disappears and the second peak either merges with the third peak or becomes a shoulder to the third peak depending on the heating rate. This phenomenon has been explained by the dual function of oxygen in PMMA decomposition. At lower temperatures, oxygen inhibits PMMA decomposition by reacting with a polymeric radical and forming a more stable new polymeric radical. At temperatures above 270 °C, this new polymeric radical decomposes and releases a more reactive radical resulting in the acceleration of PMMA decomposition [70].

Improvement in the thermal stability of PMMA nanocomposites have been on the spotlight of current research and was reported by many authors [71,72]. However, the research found MMT to have different efficiency in improving the thermal stability of PMMA, e.g. the 5%-weight-loss temperature reported by Blumstein for PMMA/OMMT was around 279 °C, which was lower than the temperature observed for PMMA–Na⁺–MMT hybrids in Kumar's study [72]. It was reported elsewhere [148] that the PMMA microcomposites with the unmodified MMT exhibited 20 wt.% loss at 280 °C while the nanocomposites showed increase in the decomposition temperature at 20 wt.% loss by 15–50 °C. Another research group [73] followed similar pathway for the synthesis but found thermal degradation temperatures of PMMA/MMT nanocomposites 10–90 °C higher in comparison with the PMMA/MMT microcomposites for the same weight loss which was attributed to the improved interaction between the PMMA and clay after the pretreatment of the clay with cetylpyridinium chloride (CPC). Similar changes in routes of thermal degradation of polymeric matrix in PMMA/MMT nanocomposites were seen when organomodifier containing vinylbenzyl groups was used [55]. As a result, the

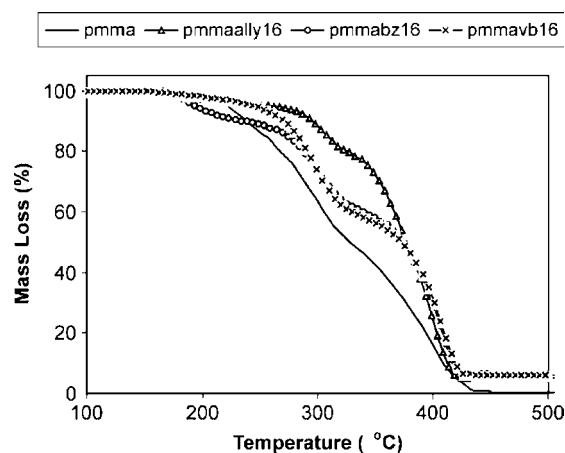


Fig. 11. TG profiles of PMMA nanocomposites [74].

onset temperature of the degradation increased by about between 50 and 100 °C for PMMA–clay nanocomposites.

In Zhu et al. work [74], three ammonium salts, hexadecylal-lyldimethyl ammonium chloride (Ally16), hexadecylvinylbenzylidimethyl ammonium chloride (VB16) and hexadecylvinylbenzylidimethyl ammonium chloride (Bz16) were synthesized and ion-exchanged onto MMT. The study reported that the presence of the clay did not affect the degradation process of PMMA; PMMA and its nanocomposites showed three degradation steps, except for the VB16 nanocomposite in which the first step disappeared. The char formation did not increase, which was consistent with previous works [51]. The TG curves (Fig. 11) for the nanocomposites showed that the initial step of the degradation, which Kashiwagi [75,76] attributed to the presence of weak links in the polymer chain, occurred at lower temperatures for Ally16 and Bz16 and was absent in VB16. The intensity of this first step decreased in the presence of the clay but it occurred at a lower temperature—this suggestion is in agreement with early studies by Blumstein and Billmeyer [77] who proposed that the clay offers some templating effect. The second and third steps in the degradation occurred at about the same point but the temperature at 50% degradation was significantly higher and the nanocomposites had enhanced thermal stability.

Referring to the GC analysis of condensable products evolved during the degradation of virgin PMMA and the PMMA/clay nanocomposite, no differences were observed [23]. Both materials underwent thermal degradation through β -scission at the chain ends (unzipping) to produce the monomer. This implies that neither a radical transfer, which is the pathway for the evolution of dimer and trimer, nor intermolecular reaction occur. This fact was connected with the stability of the radicals that are produced during the decomposition of polymer. Contrary to PS and EVA exhibiting noticeable differences in evolved products of degradation in the presence of MMT where the allylic radical in EVA and the styryl radical in styrene-containing polymers are the most stable, the radicals formed during PMMA degradation have rather low stability therefore there is small probability that radicals that are produced may undergo secondary reactions. In Qu et al. [78] it was shown that in PMMA nanocomposites synthesized by *in situ* polymerization the ratios

of termination by disproportionation in relation to recombination increased with the addition of MMT. Since the stability of the polymer formed by recombination of radical species will be around 190 °C, while polymer chains containing the unsaturated and saturated end-groups formed in disproportionation reaction should be around 255 and >300 °C, respectively, the changes in termination mechanism of free radical polymerization by MMT could be responsible for thermal stability enhancement of PMMA–clay nanocomposites.

6. Poly(vinyl chloride) (PVC)

Recent publications by Gong et al. [79] were devoted to poly(vinyl chloride) (PVC)/MMT nanocomposites that were prepared by *in situ* polymerization method. Similar to pure PVC, the nanocomposites revealed two-stage degradation in TG experiment—the first stage corresponds to the evolution of hydrogen chloride resulting in the formation of the conjugated polyene sequences, and the following stage is attributed to the thermal cracking of the carbonaceous conjugated polyene sequences (Fig. 12).

The degradation process of PVC nanocomposites was modified both in the first and the second stage. The initial mass loss occurred at lower temperatures comparing to pristine polymer. However, the temperature at maximum rate of mass loss

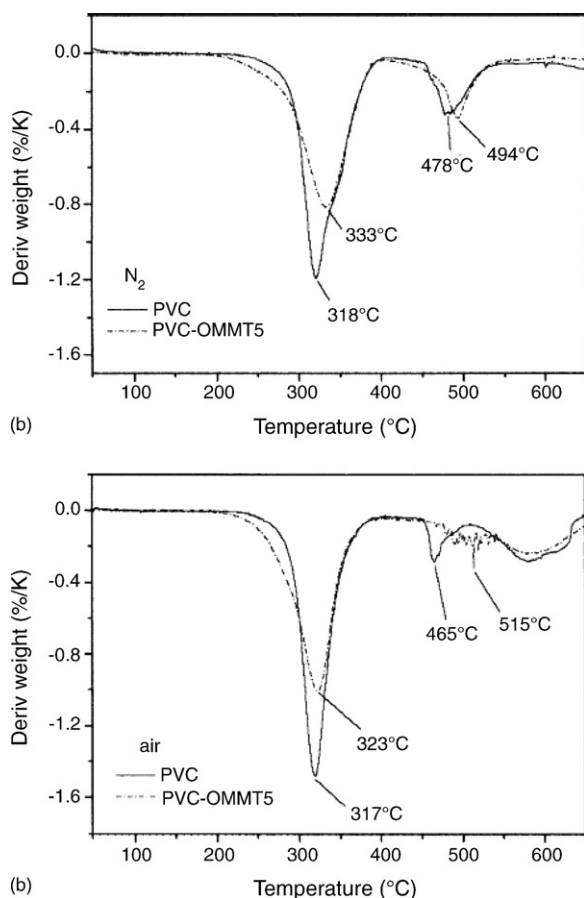


Fig. 12. DTG profiles of pure PVC and the PVC-OMMT5 in (a) nitrogen and (b) air [79].

was enhanced with respect to pure PVC and the formation of residue was noticeably increased. As in other studies on thermal stability of PVC nanocomposites with layered silicates, the presence of the quaternary ammonium (dimethyl didodecyl ammonium chloride (DDAC)) in the nanocomposites was found to be responsible for the acceleration of the polymer decomposition in the initial stage. The quaternary ammonium salt decomposed following the Hofmann degradation mechanism. It was previously proved that the presence of H⁺ and HCl may (auto)catalyze the dehydrochlorination of the PVC chains [80]. However, as the process of nanocomposite degradation proceeded, the rate of mass loss was decreasing gradually. This was more likely attributable to the presence of MMT layers offering a barrier effect to hinder the formation of small molecules and their escape from nanocomposites. Under the naked eyes, it was observed that with increasing nanofiller content the ability of nanocomposites to keep the primary shape and form a compact surface during heating was significantly enhanced, while pure PVC samples tended to expand and form porous surface. The FTIR analysis of char formed during heating confirmed the carbonaceous nature of the residue, which took an important protective role in the PVC chains degradation. Thus the decomposition rate of the nanocomposites was slowed down and the maximum decomposition temperature was increased. However, in the case of PVC nanocomposites, where rigid-rod aromatic amine modifier (Fig. 13) was applied to modify bentonite, the onset thermal decomposition temperature was slightly increased—from 295 °C for PVC to 305 °C when the OMMT content was below 1 wt.% [81].

In another development, Wan et al. [82] investigations into PVC/organic MMT nanocomposites revealed that when organic MMT loading amounted to 5 wt.%, the composites became deep yellow in colour and processing stability deteriorated, which meant that PVC began to degrade and discolour during the processing. This meant that high organic MMT contents had adverse effects on the thermal stability during melt processing, especially above 3 wt.% content. One of the explanations given was that the pure alkyl-ammonium salts began to decompose at 230 °C under nitrogen atmosphere, while organic MMT particles began to change colour from original white to yellow at around 185 °C in air. Ren et al. found that with the increase of OMMT content, the degradation of PVC became more serious leading to the decrease of mechanical properties and concluded that the OMMT content should be kept at 1 phr to realize good processing stability and mechanical properties [83]. Ivan et al. [84] have reported that PVC has the lowest thermal stability of

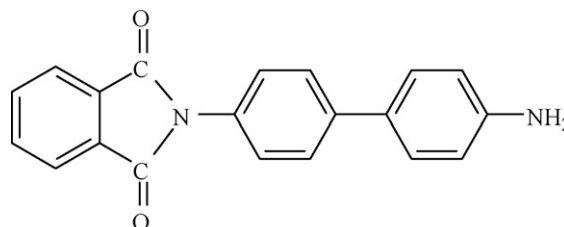


Fig. 13. Chemical structure of rigid-rod amine used for MMT modification [81].

all carbon chain polymers. Thus, the allylic and tertiary chlorines of PVC chains were the main labile ('irregular') sites, at which the decomposition process starts. When the mass loss due to dehydrochlorination reached only 0.1%, sequences of conjugated double bonds formed and resulted in discoloration of PVC.

7. Polyesters

Polyester-based nanocomposites are considered as novel materials with promising properties for e.g. packaging applications. Poly(ethylene terephthalate) (PET) nanocomposites are often prepared at elevated temperatures to above 280 °C for *in situ* intercalation and bulk processing [52,53,85,86]. Since the thermal stability of organoclays with alkyl-ammonium cations has caused severe problems during processing of PET, much research has been directed toward the preparation of organoclays that are thermally stable at high temperatures. For instance, Takekoshi et al. [87] prepared polyester/clay nanocomposites through *in situ* polymerization with high levels of dispersion and improved physical properties; however, a more commercially viable approach with conventional polymer processing led to clay poorly dispersed in polymer matrix. The researchers attributed this phenomenon to the low decomposition temperature (250 °C) of the organic modifier bound to the clay surface. Moreover, Matayabas and Turner [88] prepared PET nanocomposites by melt-compounding varying amounts of Claytone APA, a commercial high-polarity organoclay, with a 1,4-cyclohexanedimethanol modified PET. Physical mixtures of the organically modified clay and PET copolymer (*co*-PET) were dried under vacuum at 120 °C before extrusion at 280 °C. The result was a decrease in the *co*-PET inherent viscosity, indicating degradation. This degradation increased in severity as the clay content increased from 0.36 to 7 wt.%. In an attempt to compensate for the degradation, a higher-molecular weight PET was used, but unfortunately this led to more severe degradation.

An antagonistic effect of clay activity was observed in poly(butylene terephthalate) (PBT) nanocomposites [89]. The clay layers acted as a superior insulator and as a mass-transport barrier to the volatile products generated during decomposition, increasing thus the thermal stability. On the other hand, the catalytic activity centres in clay layers, such as those around hydroxyl groups, might accelerate the decomposition of the polyester [90]. As a result, the total impact of nanoadditive on thermal stability of PBT was not significant.

Further, hexadecylamine organoclay was successfully dispersed in poly(ethylene terephthalate-*co*-ethylene naphthalate) (PETN) when nanofiller content did not exceed 4 wt.% [91]. However, the tendency to form agglomerated structures in the polymer matrix at 6 wt.% clay content occurred. The observed changes in structure were simultaneously reflected in thermal stability (initial degradation temperature) confirming that hybrids with a good dispersion of organoclay are more thermally stable, though, the maximum decomposition temperatures of all the nanocomposites remained constant, regardless of the organoclay loading. Similarly to previously mentioned PET/clay nanocomposite investigations [52,53,85,86], the researchers

also emphasized the role of strong interaction between the organoclay and PETN molecules that increased the thermal resistance of nanocomposites. Such interactions were introduced by adding sodium sulfonate functionalized PBT into PET that caused exfoliation of MMT during extrusion [92]. Since high degree of exfoliation is known to be an important factor in thermal stability improvement, the proposed procedure of polymer matrix modification should be considered as a useful route towards PET nanocomposites with increased thermal resistance.

Most recently, Chang et al. [93] reported that in addition to having the same melting point and heat of melting, the PET nanocomposites with 0–3 wt.% dodecyl triphenyl phosphonium chloride modified MMT (C12PPh–MMT) showed improved thermal degradation properties. TG results showed that the initial thermal degradation temperature of the C12PPh–MMT/PET hybrid fibres increased with the amount of organoclay. The initial thermal degradation temperature at 2% mass loss was observed at 370–385 °C for clay compositions from 0 to 3 wt.% in the PET hybrids, with a maximum increase of 15 °C in the case of the 3 wt.% C12PPh–MMT/PET as compared to that for pure PET. The weight of the residue at 600 °C increased with clay loading from 0 to 3%, ranging from 1 to 21%. This enhancement of char formation was ascribed to the high heat resistance exerted by the clay itself. For 3 wt.% organoclay in the PET hybrid fibres, the overall thermal properties of the PET hybrid fibres were unchanged for different draw ratios from 1 to 16.

Studies by Liu et al. [94] indicated that inhomogeneous dispersion leads to non-systematic changes in onset temperature of degradation of poly(trimethylene terephthalate) (PTT)/18C–MMT and the PTT/12C–MMT nanocomposites, which was caused by inhomogeneous dispersion of the two organoclays. Takekoshi et al. [87] study produced PET nanocomposites with *N,N*-dimethyl-*N,N*-dioctadecylammonium treated MMT (DMDODA–MMT), which has a decomposition temperature of 250 °C. The residues were black, brittle, and tarlike resulting from DMDODA degradation under the processing conditions. PET nanocomposites compounded with 1,2-dimethyl-3-*n*-hexadecyl imidazolium treated MMT, which has a decomposition temperature of 350 °C, showed high levels of dispersion and delamination. The imidazolium-based organic modifiers were thermally stable at the processing conditions.

A different study concerning the degradation behaviour of copolyesters with phosphorous linkage in the main chain synthesized in condensation reaction of terephthalic acid (TPA), ethyleneglycol (EG) and 2-carboxyethyl(phenylphosphinic) acid (CEPP) (PET-*co*-CEPP) and phosphorous linked pendant groups (PET-*co*-DDP), where as a copolymer 9,10-dihydro-10[2,3-di(hydroxycarbonyl)propyl]10-phosphaphenanthrene-10-oxide (DDP) was used, reported the increase of the activation energy of degradation resulting from the introduction of MMT [95,96]. The synthesis of phosphorus-containing copolyesters from terephthalic acid and ethylene glycol as well as CEPP and DDP as co-monomers was meant to improve the flame retardancy; however, it turned out that PET copolymers had lower onset temperature of degradation denoted as temperature at 5% mass loss ($T_{5\%}$) and temperature of maximum mass loss (T_{\max}) than that of pure PET. For the nanocomposite

of PET copolymer (1.8 wt.% of phosphorous and 2 wt.% of inorganic MMT content), it had higher $T_{5\%}$ and T_{\max} than PET-co-DDP, suggesting that MMT can enhance the thermal stability of phosphorous-containing copolyesters. Moreover, the activation energy of decomposition determined using Kissinger, Ozawa–Flynn–Wall and Friedman methods, was increased.

8. Polyimide (PI)

Liang et al. [97] studied the thermal properties of photosensitive polyimide (PI)/MMT nanocomposites with various MMT contents. The onset thermal decomposition temperature and temperatures at 5 and 10% weight loss were increased with the increase of MMT content. For example, the onset thermal decomposition temperature assessed by TGA was increased from 515 °C for PI to 540 °C for PI/MMT nanocomposite containing 3 wt.% of MMT. MMT possessed high thermal stability and its layer structure exhibited great barrier effect to hinder the evaporation of the small molecules generated during the thermal decomposition, limiting the continuous degradation of the PI matrix.

In another research work [98], TG profiles for soluble polyimide (SPI) and soluble nanocomposite membranes prepared by chemical imidization, as measured under an air atmosphere, showed two major weight losses in the range of 100–300 °C and at 500 °C. The first noted weight loss was assigned to the evaporation of the *N*-methyl-2-pyrrolidone (NMP) solvent. The major weight loss at 500–700 °C was attributed to the structural decomposition of the polymer shifted slightly toward the higher temperature under addition of MMT. Similarly, the thermal stability of bulk PI (insoluble PI system) also showed enhancement after the incorporation of clay platelets. It was noted that the char yield of insoluble PI was significantly higher than that of SPI, indicating that the insoluble PI may show enhanced flame resistant property relative to SPI.

9. Epoxy resins

In one development, TG studies on both the onium ion intercalated clays and the epoxy/clay nanocomposites made from these clays found out that the thermal stability of the nanocomposites was not greatly compromised by the presence of the long chain organic modifier [99]. Of interest, the Jeffamine onium ions underwent facile thermal decomposition, presumably according to the Hofmann mechanism, when intercalated into MMT and fluorohectorite clays. However, there was no indication of onium ion degradation in the cured polymer/clay nanocomposites, whether the clay nanolayers were exfoliated or not. In Becker et al. [100] investigation into epoxy layered silicate nanocomposites, a slightly decreased onset temperature with increasing organoclay concentration for the tetrafunctional tetraglycidylidiaminodiphenylmethane (TGDDM) nanocomposites was observed. A similar trend was shown for the peak degradation temperature of the diglycidyl ether of bisphenol A (DGEBA) and triglycidyl *p*-amino phenol (TGAP) nanocomposites. Values for TGDDM, however,

showed some scatter around a value of about 380 °C rather than a constant trend of decreasing temperatures with clay addition. The interval between degradation onset and end showed a slight trend of broadening for the DGEBA and TGAP nanocomposites. However, this was not observed for the TGDDM nanocomposites and was not consistent with the reduced onset and peak degradation temperatures. It was noted that TG traces of resin systems with and without organoclay generally showed the same behaviour in the lower temperature regime of degradation, with the degradation of the compatibilizer starting at about 200 °C. A separate degradation of the interlayer exchanged ions was not observed, however, it was found that the organo-ion concentrations were very low, *ca.* 25–30 wt.% of the treated clay fraction. This led to assumption that the interlayer exchanged ions were well embedded or incorporated into the polymer matrix. This is in good agreement with the degradation behaviour observed for other exfoliated epoxy organoclay nanocomposites by Wang and Pinnavaia [101] and Gu and Liang [102] who recently found that onset temperatures of degradation were also lowered, especially in the case of the longer alkyl-ammonium chains. Likewise, the potential reasons leading to lower glass transition temperatures, such as low cross-link density and plasticization of the epoxy matrix by the organo-ion, were also likely to have led to greater degrees of degradation.

Becker et al. [100] studies on surface modification of MMT and thermal stability of epoxy/clay nanocomposites noted that although the total weight loss of epoxy/clay nanocomposites is not generally in direct proportion with the amount of clay added, a trend of reduced weight loss or improved char formation was observed with organoclay addition. When comparing pristine epoxy and 10% layered silicate-containing nanocomposite, the additional weight of the remaining char was in good correlation to the inorganic content of the filler given that the organoclay cations were roughly one third of the clay additive. The nanocomposites showed slight indications of reduced thermal stability, as displayed by a decreased onset in thermal degradation in the order of 5–10 °C at a clay concentration of 10%. The final char concentration was increased with increasing organoclay concentrations. The changes in thermal stability were of very low significance and it was unlikely that they would be considered as a drawback to any possible industrial application. Other work by cone calorimetry indicated that significant decreases in heat release rate occurred upon addition of nanoclays [103,104], however it is often necessary to combine the clays with other additives in order to obtain the required synergies and flame retardancy desired [105].

The influence of nanoreinforcement on thermal stability of an epoxy resin (diglycidyl ether of bisphenol A (DGEBA) polymerized with a methyl tetrahydrophthalic anhydride) was investigated by Torre et al. [106]. The overall degradation process in inert atmosphere was not strongly affected by the presence of the nanoparticles, however, the stabilizing role of MMT was visible during degradation in the presence of oxidizing gases. Furthermore, it was noticed that the presence of the accelerator (imidazole) in the nanocomposite formulation caused a decrease of the degradation performance of the material in an inert atmosphere. This phenomenon was attributed to the

effect of the surfactant, which, in the nanocomposite polymerized with imidazole, exposed more surfaces and could catalyze the decomposition.

10. Polyurethanes (PU)

The thermal degradation of polyurethanes (PU) occurs in two stages: the first stage is mainly governed by the degradation of the hard segments and the second stage correlates well with the degradation of the soft segments [107–110]. The nanocomposites with improved dispersion of organoclay showed the onset temperature of degradation (T_{onset}), the temperature of maximum decomposition rate for the first stage (T_{max1}) and that for the second stage (T_{max2}) about 10 °C higher than pristine PU. The highest thermal stability was observed for the OMMT content of 5 wt.% and its T_{onset} , T_{max1} and T_{max2} were about 30, 35 and 65 °C higher than those of pure PU. Moreover, Choi et al. [111] showed that the effect of clay as thermal insulator and mass-transport barrier on thermal stability can be increased with improving the dispersibility of organoclay in polyurethane matrix. In this study clay was modified with high molecular weight compound with hydroxyl end-groups, then dispersed in DMF and the dispersibility of organoclay in polyurethane matrix was enhanced by applying the sonication.

In Song et al. [112] study on PU-layered silicate nanocomposites based on polyether, toluene diisocyanate, diglycol (as a chain extender) and glycerine (as a cross-linking agent), a decrease in onset temperature of decomposition was ascribed to catalytic effect of OMMT. The introduction of organosilicate led to enhanced depolycondensation of macromolecular matrix in the initial stage of degradation; however, the overall rate of mass loss was diminished. An attempt was made to improve the thermal stability of PU nanocomposites at temperatures around T_{onset} by introducing the melamine polyphosphate (MPP). Thermal degradation of MPP takes place at about 360 °C—it releases NH_3 and H_2O and generates highly cross-linked unidentified polyphosphoric acid derivatives containing P–N linkages. Although there was an obvious synergic effect between the retardance of the thermal decomposition and enhancement of carbonaceous char formation, which occurred between OMMT and MPP, the catalytic effect of OMMT was still found. It was suggested that catalysis of the phosphoric acid also accelerated the depolycondensation reaction.

In another development, PU/MMT nanocomposites, based on thermally stable, aromatic amine modifier containing active groups (methylene-bis-*ortho*-chloroaniline, (MOCA)), were synthesized by intercalative polymerization [113]. The cured hybrid exhibited higher thermal stability and better mechanical strength than pure PU or PU/cetyltrimethylammonium-bromide (CTAB)-modified MMT (PU/C16-MMT). The main reason for different behaviour of nanocomposites was the different structure of the modifiers. The aromatic chain of MOCA has higher thermal stability compared to alkyl chain of CTAB. On the other hand, compared with the CTAB, MOCA modifier, as a chain extender, could react with the pre-polyurethane matrix, further strengthening the interaction between inorganic and organic phase. As a result, modifier molecules (MOCA) in the PU/MMT

were connected with PU by covalent bonds and become a constituent part of the polyurethane, while the alkyl chain of CTAB and PU permeated with each other and formed a thin interface in the PU/C16-MMT. Lastly, Takeichi and Guo [114] reported the improvement in thermal stability of poly(urethane-benzoxazine) (PU-Pa) nanocomposites with OMMT that was suggested to be based on two effects: first, part of the thermally decomposed volatiles was captured by OMMT; second, the efficient cure of benzoxazine monomer (Pa), from the catalytic effect of OMMT on the ring-opening polymerization, resulted in higher cross-link density of PU-Pa.

11. Ethylene–propylene–diene terpolymer (EPDM)

The role of thermal stability of organic modifier during preparation of nanocomposites was also pointed by Acharya et al. in a work on ethylene–propylene–diene terpolymer (EPDM) nanocomposites [115]. Hexadecyl ammonium salt was chosen as an organic modifier. The resulted nanocomposites (obtained by a solution blending method) exhibited exfoliated structure at clay content below 2 wt.% and mostly intercalated structure at higher contents of organosilicates. Interestingly, in intercalated nanocomposites a shift of basal 2θ peak of organophilic clay in the EPDM matrix from 4.5° to 5.5° was observed, which reflected the reduction of the silicate gallery distance. According to the researchers, such a decrease in d -spacing of silicate layers of MMT dispersed in the EPDM matrix could be attributed to the partial decomposition of the hexadecyl ammonium and expulsion of the ammonium salt, leading to the collapse of the organoclay layered structure. This hypothesis was confirmed by XRD analysis of the organomodified clay that underwent thermal treatment, where the basal reflection peak was also similarly shifted. The work observed significant improvement in thermal stability corresponding to the onset temperature of degradation (T_{onset}) for 2 wt.% mass loss that was raised from 325 °C for neat EPDM to 375 °C for 8 wt.% OMMT content in EPDM nanocomposites. This was ascribed to the presence of silicate layers, hindering the formation of small molecules, resulting from thermal decomposition, and simultaneously resisting their movement and desorption from the surface. Also the restriction of the thermal motion of EPDM segments could bring higher thermal resistance of hybrid material. Since the interfacial interactions play an important role in that process, the coexistence of intercalated and exfoliated silicate layers in the EPDM matrix, which increased the Si–O–C interactions, could be profitable. Furthermore, it was noticed that the final thermal decomposition temperature (T_f) at about 460 °C remains more or less the same, irrespective of the OMMT content in EPDM, suggesting that silicate layers were incapable of holding the polymer chains within themselves.

12. Poly(vinyl alcohol) (PVA)

Investigations in to thermal degradation of poly(vinyl alcohol) (PVA)–clay nanocomposite materials found out that major weight losses were observed in the range of 200–500 °C for pure PVA and its nanocomposites, which might have corre-

sponded to the structural decomposition of the polymer [116]. Evidently, the thermal decomposition of those hybrid materials shifted slightly toward the higher temperature range than that of PVA, which confirmed the enhancement of thermal stability of intercalated polymer. After 600 °C, the main products were mainly the inorganic residue (i.e. Al₂O₃, MgO, SiO₂). From the amount of the residue at 900 °C, the inorganic contents in the original nanocomposite materials could be obtained.

Chang et al. [117] also observed slight enhancement in the thermal stability for PVA nanocomposites—the initial decomposition temperature at a 2 wt.% loss for the hybrids was 7–15 °C higher than that of pure PVA. The analysis of the amount of char formed during degradation lead to the conclusion that the organic alkyl groups of alkyl-ammonium ion-exchanged clays thermally decomposed more easily than hybrids of sodium clays did.

13. Polylactide (PLA)

Different thermal behaviour in inert and oxidative conditions of polylactide/MMT nanocomposites was reported by Pluta et al. [118]. Under helium degradation temperature of nanocomposites was increased by about 10 °C, while increase by 25 °C was observed under air. On the other hand, the microcomposites exhibited similar thermal resistance both in helium and air. Therefore, the improved thermal stability of nanocomposite materials was ascribed to the difference in morphologic features of both materials. TG analysis performed on the poly(L-lactide)/OMMT by Paul et al. [119] showed the weight loss due to the volatilisation of degradation by-products was monitored as a function of temperature increased, and also showed an increase of the thermal stability of the polymer matrix, when filled with a small amount of nanoclay as low as 3 wt.%. Depending on the type of filler (the presence and nature of the alkyl-ammonium cations, length of the alkyl chain or functionality of the ammonium cation), this effect was pronounced in nanocomposites containing Na⁺-MMT, triggering greater thermal stability improvement where the main process of degradation was shifted towards higher temperature by 40 °C. These characteristics were related to the structure of the nanocomposite and have already been reported for other layered silicate nanocomposites based on matrices such as PA 6 [120], PS [51], ethylene-vinyl acetate copolymers [121] or poly(L-caprolactone) [122] filled with various types of OMMTs. In fact, the layers of organomodified phyllosilicates were thought to increase the diffusion pathway of the combustion by-products, as they are impermeable to such components [123].

14. Summary

In a number of investigations montmorillonite was showed to significantly affect the thermal stability of polymers as well as alter the structure and concentration of decomposition products both in evolved gases and condensed phase. The advantageous influence of clay on thermal stability of polymers clearly depends on the degree of intercalation/exfoliation of clay layers—the better dispersion of nanofiller is achieved,

the more significant enhancement of thermal resistance could be expected.

Two opposing activities of the organoclay occurred in some polymeric nanocomposites influencing the thermal stability of material—one was increasing a barrier properties ('labyrinth effect') and insulating properties to heat transport of nanocomposite that should improve the thermal stability, and the other is the catalytic effect towards the degradation of the polymer matrix which would decrease the thermal stability. The products of thermal decomposition of organic modifier influence the polymer properties, for example the acidic sites occurring on MMT layer after volatilisation of organomodifier are able to accelerate the decomposition of polymer. Furthermore, the compounds that are absorbed on MMT surface, such as water, for some polymers (e.g. polyamides, polyesters, polyurethanes) could initiate hydrolysis. Low molecular weight compounds absorbed in polymer matrix may cause deterioration of the mechanical performance of composite material.

Moreover, the results of recent systematic studies showed that the clay activity towards thermal stabilization of polymers depends on the intrinsic properties of polymer matrix, and more specifically, on the routes of polymer degradation. In a case of polymeric nanocomposites that exhibited improved thermal stability and/or fire retardancy significant intermolecular reactions occurred, such as inter-chain aminolysis/acidolysis, radical recombination and hydrogen abstraction. New products in gaseous and condensed phase are then formed following additional degradation pathways. It can be accepted that in the presence of MMT layers acting as a barrier to heat and mass transport first more extensive random scission of polymer chain occurs due to superheated conditions in the condensed phase. Then chemical species, trapped between MMT layers, have more opportunity to undergo further intermolecular reactions, such as radical recombination. The intermolecular reactions lead to the formation of complex compounds thus lowering the volatilisation rate and favour the char formation process. Interestingly, it was showed that the influence of MMT on the thermal stability and fire retardancy of polymers depends on the degradation pathways of the polymer—some of them could be promoted in the presence of MMT. For polymers that undergo thermal degradation according to the radical mechanism, the different efficiency of MMT in improving thermal behaviour can be connected with the stability of radical compounds produced by the polymer—the radical species with higher stability are more probable to undergo radical recombination reactions.

Different effects were observed for thermo-oxidation and degradation in pyrolytic conditions. On the basis of observed changes in degradation routes of polymers it was found that the 'labyrinth effect' of dispersed MMT is responsible for restricted diffusion of oxygen into polymer matrix and causes pyrolytic-like conditions inside nanostructured composite material.

References

- [1] K. Pielichowski, J. Njuguna, *Thermal Degradation of Polymeric Materials*, Rapra, Shawbury, 2005.
- [2] J. Pielichowski, K. Pielichowski, *J. Therm. Anal.* 43 (1995) 505.

- [13] S.D. Burnside, E.P. Giannelis, *Chem. Mater.* 7 (1995) 1597.
- [14] J. Lee, T. Takekoshi, E.P. Giannelis, *Mater. Res. Soc. Symp. Proc.* 457 (1997) 513.
- [15] A. Blumstein, *J. Polym. Sci. Part A-1* 3 (1965) 2665.
- [16] H. Qin, Q. Su, S. Zhang, B. Zhao, M. Yang, *Polymer* 44 (2003) 7533.
- [17] F. Ide, A. Hasegawa, *J. Appl. Polym. Sci.* 18 (1974) 963.
- [18] M. Zanetti, G. Camino, P. Peichert, R. Mülhaupt, *Macromol. Rapid Commun.* 22 (2001) 176.
- [19] A. Leszczyńska, K. Pielichowski, J. Njuguna, J.R. Banerjee, *Thermochim. Acta*, in press.
- [10] C. Ding, D. Jia, H. He, B. Guo, H. Hong, *Polym. Test.* 24 (2005) 94.
- [11] Y.-Q. Zhang, J.-H. Lee, J.M. Rhee, K.Y. Rhee, *Compos. Sci. Technol.* 64 (2004) 1383.
- [12] Y.-Q. Zhang, J.-H. Lee, H.-J. Jang, C.-W. Nah, *Compos. Part B: Eng.* 35 (2004) 133.
- [13] J. Zhang, C.A. Wilkie, *Polym. Degrad. Stab.* 83 (2004) 301.
- [14] F.-C. Chiu, S.-M. Lai, J.-W. Chen, P.-H. Chu, *J. Polym. Sci. Part B: Polym. Phys.* 42 (2004) 4139.
- [15] C.M.L. Preston, G. Amarasinghe, J.L. Hopewell, R.A. Shanks, Z. Mathys, *Polym. Degrad. Stab.* 84 (2004) 533.
- [16] M. Zanetti, G. Camino, R. Thomann, R. Mülhaupt, *Polymer* 42 (2001) 4501.
- [17] H. Qin, S. Zhang, C. Zhao, M. Yang, *J. Polym. Sci. Part B: Polym. Phys.* 43 (2005) 3713.
- [18] S.M. Lomakin, I.L. Dubnikova, S.M. Berezina, G.E. Zaikov, *Polym. Int.* 54 (2005) 999.
- [19] I. Mita, in: H.H.G. Jellinek (Ed.), *Aspects of Degradation and Stabilization of Polymers*, Elsevier, Amsterdam, 1978.
- [20] J.L. Philippart, F. Posada, J.L. Gardette, *Polym. Degrad. Stab.* 49 (1995) 285.
- [21] A. Tidjani, *Polym. Degrad. Stab.* 87 (2005) 43.
- [22] M. Poutsma, *Macromolecules* 36 (2003) 8931.
- [23] B.N. Jang, M. Costache, C.A. Wilkie, *Polymer* 46 (2005) 10678.
- [24] J.H. Adams, *J. Polym. Sci. Part A-1* 8 (1970) 1077.
- [25] J. Zhang, C.A. Wilkie, *Polym. Degrad. Stab.* 80 (2003) 163.
- [26] X. Zheng, C.A. Wilkie, *Polym. Degrad. Stab.* 82 (2003) 441.
- [27] C. Zhao, M. Yang, M. Feng, *Chem. J. Chin. Univ.* 24 (2003) 928.
- [28] C. Zhao, M. Feng, F. Gong, M. Yang, *Chin. J. Chem.* 21 (2003) 1031.
- [29] C. Zhao, H. Qin, F. Gong, M. Feng, S. Zhang, M. Yang, *Polym. Degrad. Stab.* 87 (2005) 183.
- [30] G. Camino, R. Sgobbi, C. Colombier, C. Scelza, *Fire Mater.* 24 (2000) 85.
- [31] M.C. Costache, D.D. Jiang, C.A. Wilkie, *Polymer* 46 (2005) 6947.
- [32] K.P. Pramoda, T. Liu, Z. Liu, C. He, H.-J. Sue, *Polym. Degrad. Stab.* 81 (2003) 47.
- [33] B.J. Holland, J.N. Hay, *Polym. Int.* 49 (2000) 943.
- [34] S.-J. Park, D.-I. Seo, J.-R. Lee, *J. Coll. Interf. Sci.* 251 (2002) 160.
- [35] J.W. Gilman, T. Kashiwagi, J.E.T. Brown, S. Lomakin, *SAMPE J.* 33 (1997) 40.
- [36] Z.H. Liu, T.X. Liu, C.B. He, H.-J. Sue, A.F. Yee, *Proceedings of the ACS National Meeting, Orlando, USA, April 7–11, 2002*.
- [37] S.V. Levchik, E.D. Weil, M. Lewin, *Polym. Int.* 48 (1999) 532–557.
- [38] R.D. Davis, J.W. Gilman, D.L. VanderHart, *Polym. Degrad. Stab.* 79 (2003) 111.
- [39] B.N. Jang, C.A. Wilkie, *Polymer* 46 (2005) 3264.
- [40] T. Kashiwagi, R.H. Harris Jr., X. Zhang, R.M. Briber, B.H. Cipriano, S.R. Raghavan, W.H. Awad, J.R. Shields, *Polymer* 45 (2004) 881.
- [41] F. Dąbrowski, S. Bourbigot, R. Delobel, M. Le Bras, *Eur. Polym. J.* 36 (2000) 273.
- [42] T. Liu, K.P. Lim, W.C. Tjiu, K.P. Pramoda, Z.-K. Chen, *Polymer* 44 (2003) 3529.
- [43] S. Bourbigot, J.W. Gilman, C.A. Wilkie, *Polym. Degrad. Stab.* 84 (2004) 483.
- [44] N. Grassie, G. Scott, *Polymer Degradation and Stabilization*, Cambridge University Press, Cambridge, 1985.
- [45] K. Pielichowski, A. Puszynski, J. Pielichowski, *Polym. J.* 26 (1994) 822.
- [46] K. Pielichowski, L. Stoch, *J. Therm. Anal.* 45 (1995) 1239.
- [47] K. Chen, M.A. Susner, S. Vyazovkin, *Macromol. Rapid Commun.* 26 (2005) 690.
- [48] S. Vyazovkin, I. Dranca, X. Fan, R. Advincula, *J. Phys. Chem. B* 108 (2004) 11672.
- [49] S. Vyazovkin, I. Dranca, X. Fan, R. Advincula, *Macromol. Rapid Commun.* 25 (2004) 498.
- [50] J.W. Gilman, C.L. Jackson, A.B. Morgan, *Chem. Mater.* 12 (2000) 1866.
- [51] J. Zhu, C.A. Wilkie, *Polym. Int.* 49 (2000) 1158.
- [52] J. Zhu, A.B. Morgan, F.J. Lamelas, C.A. Wilkie, *Chem. Mater.* 13 (2001) 3774.
- [53] J. Zhu, F.M. Uhl, A.B. Morgan, C.A. Wilkie, *Chem. Mater.* 13 (2001) 4649.
- [54] Z.M. Wang, T.C. Chung, J.W. Gilman, E. Manias, *J. Polym. Sci. Part B: Polym. Phys.* 41 (2003) 3173.
- [55] S. Su, C.A. Wilkie, *J. Polym. Sci. Part A: Polym. Chem.* 41 (2003) 1124.
- [56] D. Wang, C.A. Wilkie, *Polym. Degrad. Stab.* 82 (2003) 309.
- [57] M.T. Sousa Pessoa De Amorim, C. Bouster, P. Vermande, J. Veron, *J. Anal. Appl. Pyrol.* 3 (1981) 19.
- [58] U.K.O. Schroeder, K.H. Ebert, A.W. Hamielec, *Macromol. Chem.* 185 (1984) 991.
- [59] I.C. McNeill, M. Zulfiqar, T. Kousar, *Polym. Degrad. Stab.* 28 (1990) 131.
- [60] A. Guyot, *Polym. Degrad. Stab.* 15 (1986) 219.
- [61] M. Guaita, O. Chiantore, L. Costa, *Polym. Degrad. Stab.* 12 (1985) 315.
- [62] B.N. Jang, C.A. Wilkie, *Polymer* 46 (2005) 2933.
- [63] S. Wang, Y. Hu, L. Song, Z. Wang, Z. Chen, W. Fan, *Polym. Degrad. Stab.* 77 (2002) 423.
- [64] Z. Zhang, L. Zhang, Y. Li, H. Xu, *Polymer* 46 (2005) 129.
- [65] L.-L. Chu, S.K. Anderson, J.D. Harris, M.W. Beach, A.B. Morgan, *Polymer* 45 (2004) 4051.
- [66] N. Grassie, D.R. Bain, *J. Polym. Sci. Part A-1* 8 (1970) 2679.
- [67] B.N. Jang, C.A. Wilkie, *Polymer* 46 (2005) 9702.
- [68] J. Fossey, D. Lefort, J. Sorba, *Free Radicals in Organic Chemistry*, Wiley, New York, 1995.
- [69] J.M. Hwu, G.J. Jiang, Z.M. Gao, W. Xie, W.P. Pan, *J. Appl. Polym. Sci.* 83 (2002) 1702.
- [70] J.D. Peterson, S. Vyazovkin, C.A. Wight, *J. Phys. Chem. B* 103 (1999) 8087.
- [71] A. Blumstein, *J. Polym. Sci. Part A: Gen. Pap.* 3 (1965) 2665.
- [72] S. Kumar, J.P. Jog, U. Natarajan, *J. Appl. Polym. Sci.* 89 (2003) 1186.
- [73] H. Essawy, A. Badran, A. Youssef, A. El-Fetoh, A. El-Hakim, *Polym. Bull.* 53 (2004) 9.
- [74] J. Zhu, P. Start, K.A. Mauritz, C.A. Wilkie, *Polym. Degrad. Stab.* 77 (2002) 253.
- [75] T. Kashiwagi, A. Inaba, J.E. Brown, K. Hatada, T. Kitayama, E. Masuda, *Macromolecules* 19 (1986) 2160.
- [76] J.W. Gilman, T. Kashiwagi, E.P. Giannelis, E. Manias, S. Lomakin, J.D. Lichtenham, in: M. LeBras, G. Camino, S. Bourbigot, R. Delobel (Eds.), *Fire Retardancy of Polymers: The Use of Intumescence*, Royal Society of Chemistry London, 1998.
- [77] A. Blumstein, F.W. Billmeyer, *J. Polym. Sci. Part A-2* 4 (1966) 465.
- [78] X. Qu, T. Guan, G. Liu, Q. She, L. Zhang, *J. Appl. Polym. Sci.* 97 (2005) 348.
- [79] F. Gong, M. Feng, C. Zhao, S. Zhang, M. Yang, *Polym. Degrad. Stab.* 84 (2004) 289.
- [80] G. Scott, M. Tahan, *Eur. Polym. J.* 11 (1975) 535.
- [81] Z.-M. Liang, C.-Y. Wan, Y. Zhang, P. Wei, J. Yin, *J. Appl. Polym. Sci.* 92 (2004) 567.
- [82] C. Wan, X. Qiao, Y. Zhang, Y. Zhang, *Polym. Test.* 22 (2003) 453.
- [83] T. Ren, J. Yang, Y. Huang, J. Ren, Y. Liu, *Polym. Compos.* 27 (2006) 55.
- [84] B. Ivan, T. Kelen, F. Tudos, *Degradation and Stabilization of Polymers*, Elsevier, New York, 1989.
- [85] C. Saujanya, Y. Imai, H. Tateyama, *Polym. Bull.* 49 (2002) 69.
- [86] C.H. Davis, L.J. Mathias, J.W. Gilman, D.A. Schiraldi, J.R. Shields, P. Trulove, T.E. Sutto, H.C. Delong, *J. Polym. Sci. Part B: Polym. Phys.* 40 (2002) 2661.
- [87] T. Takekoshi, F.F. Khouri, J.R. Campbell, T.C. Jordan, K.H. Dai, *US Patent* 5,530,052 (1996).

- [88] J.C. Matayabas Jr., S.R. Turner, in: T.J. Pinnavaia, G.W. Beall (Eds.), *Polymer–Clay Nanocomposites*, Wiley, New York, 2001.
- [89] J. Xiao, Y. Hu, Z. Wang, Y. Tang, Z. Chen, W. Fan, *Eur. Polym. J.* 41 (2005) 1030.
- [90] W. Xie, Z.M. Gao, W.P. Pan, D. Hunter, A. Singh, R.A. Vaia, *Chem. Mater.* 13 (2001) 2979.
- [91] J.-H. Chang, D.-K. Park, *J. Polym. Sci. Part B: Polym. Phys.* 39 (2001) 2581.
- [92] B.J. Chisholm, R.B. Moore, G. Barber, F. Khouri, A. Hempstead, M. Larsen, E. Olson, J. Kelley, G. Balch, J. Caraher, *Macromolecules* 35 (2002) 5508.
- [93] J.-H. Chang, S.J. Kim, Y.L. Joo, S. Im, *Polymer* 45 (2004) 919.
- [94] Z. Liu, K. Chen, D. Yan, *Polym. Test.* 23 (2004) 323.
- [95] H. Zhao, Y.Z. Wang, D.Y. Wang, B. Wu, D.Q. Chen, X.L. Wang, E. Al, *Polym. Degrad. Stab.* 80 (2003) 135.
- [96] D.-Y. Wang, Y.-Z. Wang, J.-S. Wang, D.-Q. Chen, Q. Zhou, B. Yang, W.-Y. Li, *Polym. Degrad. Stab.* 87 (2005) 171.
- [97] Z.-M. Liang, J. Yin, J.-H. Wu, Z.-X. Qiu, F.-F. He, *Eur. Polym. J.* 40 (2004) 307.
- [98] J.-M. Yeh, Ch.-L. Chen, T.-H. Kuo, W.-F. Su, H.-Y. Huang, D.-J. Liaw, H.-Y. Lu, Ch.-F. Liu, Y.-H. Yu, *J. Appl. Polym. Sci.* 92 (2004) 1072.
- [99] C.S. Triantafillidis, P.C. Le Baron, T.J. Pinnavaia, *J. Solid State Chem.* 167 (2002) 354.
- [100] O. Becker, R.J. Varley, G.P. Simon, *Eur. Polym. J.* 40 (2004) 187.
- [101] Z. Wang, J.T. Pinnavaia, *Chem. Mater.* 10 (1998) 1820.
- [102] A. Gu, G. Liang, *Polym. Degrad. Stab.* 80 (2003) 383.
- [103] J. Gilman, T. Kashiwagi, J. Brown, S. Lomakin, E. Giannelis, *Proceedings of the 43rd International SAMPE Symposium*, Anaheim, USA, May 31–June 4, 1998.
- [104] J.W. Gilman, *Appl. Clay Sci.* 15 (1999) 31.
- [105] M. Zanetti, G. Camino, D. Canavese, A.B. Morgan, F.J. Lamelas, C.A. Wilkie, *Chem. Mater.* 14 (2002) 189.
- [106] L. Torre, E. Frulloni, J.M. Kenny, C. Manferti, G. Camino, *J. Appl. Polym. Sci.* 90 (2003) 2532.
- [107] J. Njuguna, K. Pielichowski, *Adv. Eng. Mater.* 6 (2004) 193.
- [108] Z.S. Petrović, Z. Zavargo, J.H. Flynn, W.J. Macknight, *J. Appl. Polym. Sci.* 51 (1994) 1087.
- [109] J. Njuguna, K. Pielichowski, *Adv. Eng. Mater.* 5 (2003) 769.
- [110] J. Njuguna, K. Pielichowski, *Adv. Eng. Mater.* 6 (2004) 204.
- [111] W.J. Choi, S.H. Kim, Y.J. Kim, S.C. Kim, *Polymer* 45 (2004) 6045.
- [112] L. Song, Y. Hu, Y. Tang, R. Zhang, Z. Chen, W. Fan, *Polym. Degrad. Stab.* 87 (2005) 111.
- [113] J. Xiong, Y. Liu, X. Yang, X. Wang, *Polym. Degrad. Stab.* 86 (2004) 549.
- [114] T. Takeichi, Y. Guo, *J. Appl. Polym. Sci.* 90 (2003) 4075.
- [115] H. Acharya, M. Pramanik, S.K. Srivastava, A.K. Bhowmick, *J. Appl. Polym. Sci.* 93 (2004) 2429.
- [116] Y.-H. Yu, C.-Y. Lin, J.-M. Yeh, W.-H. Lin, *Polymer* 44 (2003) 3553.
- [117] J.-H. Chang, T.-G. Jang, K.J. Ihn, W.-K. Lee, G.S. Sur, *J. Appl. Polym. Sci.* 90 (2003) 3208.
- [118] M. Pluta, A. Gałęski, M. Alexandre, M.-A. Paul, P. Dubois, *J. Appl. Polym. Sci.* 86 (2002) 1497.
- [119] M.-A. Paul, M. Alexandre, P. Degee, C. Henrist, A. Rulmont, P. Dubois, *Polymer* 44 (2003) 443.
- [120] L. Liu, Z. Qi, X. Zhu, *J. Appl. Polym. Sci.* 71 (1999) 1133.
- [121] M. Alexandre, G. Beyer, C. Henrist, R. Cloots, A. Rulmont, R. Jérôme, P. Dubois, *Macromol. Rapid Commun.* 22 (2001) 643.
- [122] N. Pantoustier, M. Alexandre, P. Degée, C. Calberg, R. Jérôme, C. Henrist, R. Cloots, A. Rulmont, P. Dubois, *e-Polymers* (2001) 009.
- [123] M. Zanetti, G. Camino, R. Mülhaupt, *Polym. Degrad. Stab.* 74 (2001) 413.
- [124] H. Zhai, W. Xu, H. Guo, Z. Zhou, S. Shen, Q. Song, *Eur. Polym. J.* 40 (2004) 2539.
- [125] J. Zhang, D.D. Jiang, C.A. Wilkie, *Polym. Degrad. Stab.* 91 (2006) 298.
- [126] L. Qiu, W. Chen, B. Qu, *Polymer* 47 (2006) 922.
- [127] S. Su, D.D. Jiang, C.A. Wilkie, *Polym. Degrad. Stab.* 83 (2004) 321.
- [128] Y. Tang, Y. Hu, L. Song, R. Zong, Z. Gui, Z. Chen, W. Fan, *Polym. Degrad. Stab.* 82 (2003) 127.
- [129] Y. Tang, Y. Hu, S. Wang, Z. Gui, Z. Chen, W. Fan, *Polym. Adv. Technol.* 14 (2003) 733.
- [130] F. Bertini, M. Canetti, G. Audisio, G. Costa, L. Falqui, *Polym. Degrad. Stab.* 91 (2006) 600.
- [131] C. Wang, Q. Wang, X. Chen, *Macromol. Mater. Eng.* 290 (2005) 920.
- [132] S. Su, D.D. Jiang, C.A. Wilkie, *Polym. Degrad. Stab.* 83 (2004) 333.
- [133] G. Chigwada, D.D. Jiang, C.A. Wilkie, *Thermochim. Acta* 436 (2005) 113.
- [134] J. Zhang, D.D. Jiang, C.A. Wilkie, *Polym. Degrad. Stab.* 91 (2006) 358.
- [135] D. Wang, C.A. Wilkie, *Polym. Degrad. Stab.* 80 (2003) 171.
- [136] G. Chigwada, D. Wang, D.D. Jiang, C.A. Wilkie, *Polym. Degrad. Stab.* 91 (2006) 755.
- [137] X. Zheng, D.D. Jiang, D. Wang, C.A. Wilkie, *Polym. Degrad. Stab.* 91 (2006) 289.
- [138] X. Zheng, D.D. Jiang, C.A. Wilkie, *Thermochim. Acta* 435 (2005) 202.
- [139] P. Jash, C.A. Wilkie, *Polym. Degrad. Stab.* 88 (2005) 401.
- [140] J.-H. Chang, S.J. Kim, *Polym. Bull.* 52 (2004) 289.
- [141] Y. Li, J. Ma, Y. Wang, B. Liang, *J. Appl. Polym. Sci.* 98 (2005) 1150.
- [142] C.-F. Ou, *J. Appl. Polym. Sci.* 89 (2003) 3315.
- [143] Z.-M. Liang, J. Yin, *J. Appl. Polym. Sci.* 90 (2003) 1857.
- [144] A. Pattanayak, S.C. Jana, *Polymer* 46 (2005) 5183.
- [145] J.-H. Chang, Y.U. An, *J. Polym. Sci. Part B: Polym. Phys.* 40 (2002) 670.
- [146] Y.I. Tien, K.H. Wei, *J. Appl. Polym. Sci.* 86 (2002) 1741.
- [147] J.-H. Chang, K.M. Park, D. Cho, H.S. Yang, K.J. Ihn, *Polym. Eng. Sci.* 41 (2001) 1514.
- [148] X. Huan, W.J. Brittain, *Macromolecules* 34 (2001) 3255.